Supplementary material

S1. Table of sample locations

Sample	Rock type	Location	Region	GPS	U-Pb/ Nd
12	Quartzo-feldspathic metasediment	Takdah	Darjeeling hills, W. Bengal	N27 00.810 E88 25.369	U-Pb
32	Orthogneiss	Rongli- Lingtam	East Sikkim	N27 13.200 E88 43.786	U-Pb
38x	Quartzo-feldspathic metasediment	Paiyong, nr.Kalimpong	Kalimpong hills, W.Bengal	N27 06.128 E88 32.542	U-Pb
49	Orthogneiss	Tashi viewpoint, Gangtok	North Sikkim	N27 21.472 E88 37.403	U-Pb
51x	garnet-staurolite-kyanite schist	Gangtok-Mangan waterwheel	North Sikkim	N27 25.159 E88 37.530	Nd
53	garnet schist	Rang Rang	North Sikkim	N27 27.958 E88 31.473	Nd
57	Garnet fibrolite schist	Myang	North Sikkim	N27 31.642 E88 36.396	Nd
58	Orthogneiss	Manul	North Sikkim	N27 30.864 E88 34.964	U-Pb
59a	garnet-staurolite-kyanite schist	Singhik	North Sikkim	N27 30.956 E88 33.454	Nd
64a	sillimanite mica schist	Toong	North Sikkim	N27 33.637 E88 39.152	Nd
66	garnet gneiss	Chungthang-Lachung	North Sikkim	N27 37.233 E88 39.729	Nd
82	garnet mica schist	Pedong	Kalimpong hills-W.Bengal	N27 07.153 E88 35.209	Nd
94	garnet mica	Sangkalang	North Sikkim	N27 31.965 E88	Nd

	schist			30.591	
97	mica schist	Mangan petrol pump	North Sikkim	N27 29.534 E88 31.686	Nd
106	garnet mica schist	Rishop	Kalimpong hills- W.Bengal	N27 06.357 E88 38.734	Nd
115	Orthogneiss	Lava	Kalimpong hills, W.Bengal	N27 04.993 E88 40.191	U-Pb
123	fibrolite mica schist	Neora valley	Kalimpong hills- W.Bengal	N27 06.170 E88 40.405	Nd
147	kyanite-fibrolite schist	Lava road	Kalimpong hills- W.Bengal	N27 01.742 E88 42.062	Nd
149	chlorite-muscovite phyllite	Lava road	Kalimpong hills- W.Bengal	N27 00.124 E88 41.876	Nd
156	garnet mica schist	Lolaygoan	Kalimpong hills- W.Bengal	N27 04.290 E88 36.886	Nd
159	fibrolite mica schist	Lolaygoan	Kalimpong hills- W.Bengal	N27 01.117 E88 33.829	Nd
161	Quartzite	Lolaygoan	Kalimpong hills, W.Bengal	N27 03.395 E88 34.359	U-Pb
203	Quartz-rich metasediment	Dikchu	North/ Central Sikkim	N27 24.794 E88 30.940	U-Pb
211	Quartzite	Rongli Dam	East Sikkim	N27 12.332 E88 42.810	U-Pb
214x	garnet-kyanite-sillimanite gneiss	Yoksom	West Sikkim	N27 21.362 E88 13.237	Nd

233	Orthogneiss	Pelling-Yoksom road	West Sikkim	N27 18.405 E88 11.967	U-Pb
245	Orthogneiss	Pelling-Dentam road	West Sikkim	N27 16.669 E88 10.075	U-Pb
246a	sillimanite mica schist	Dentam	West Sikkim	N27 16.456 E88 10.333	Nd
267	garnet-2nd sillimanite gneiss	Kabur	West Sikkim	N27 15.512 E88 09.255	Nd
275	garnet fibrolite schist	Pelling	West Sikkim	N27 18.308 E88 12.495	Nd
278	garnet-staurolite-kyanite schist	Pelling	West Sikkim	N27 18.015 E88 13.286	Nd
280	Orthogneiss	Lachung	North Sikkim	N27 41.159 E88 44.312	U-Pb
292	Quartzite	Chungthang	North Sikkim	N27 36.094 E88 38.741	U-Pb

S2. Photomicrographs of samples

12- quartzo-feldspathic metasedimentary rock

PPL- 28 mm field of view

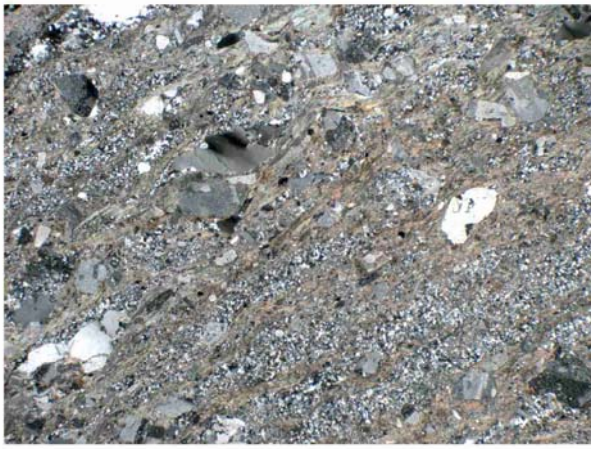

XPL- 28 mm field of view

32- orthogneiss

PPL- 25 mm field of view

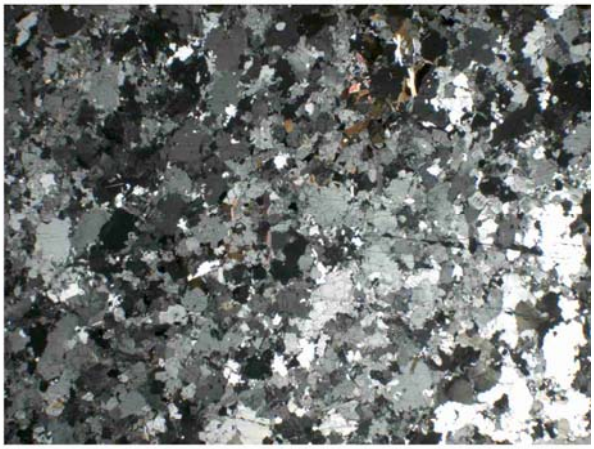

XPL- 25 mm field of view

32- melt textures

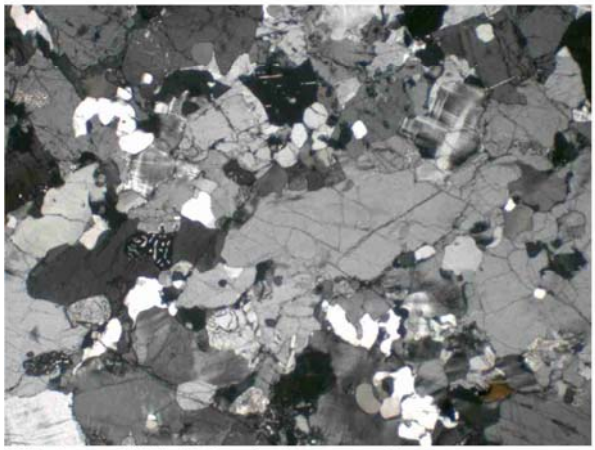

XPL- 4 mm field of view (melt textures)

38x- quartzo-feldspathic metasedimentary rock

PPL- 14 mm field of view

XPL- 14 mm field of view

49- orthogneiss (micaceous)

PPL- 28 mm field of view

XPL- 28 mm field of view

51x- garnet-staurolite-kyanite schist

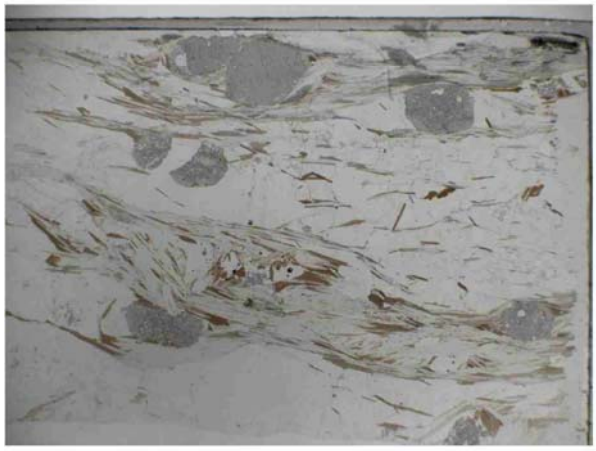

PPL- 26 mm field of view

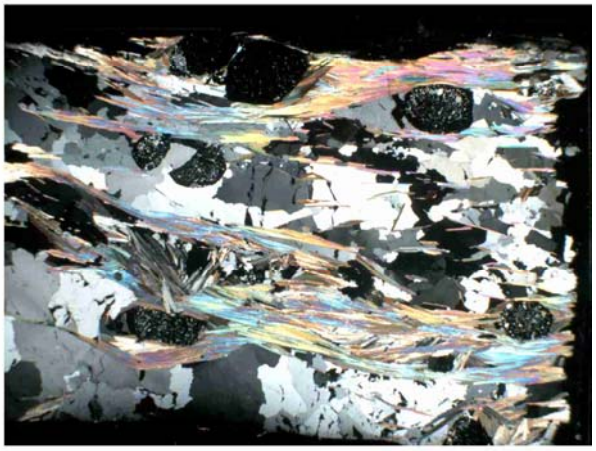

XPL- 26 mm field of view

51x- key minerals

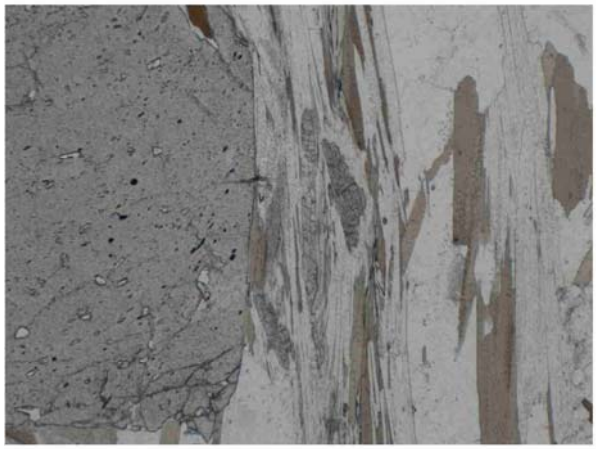

PPL- 3.5 mm field of view (garnet + kyanite)

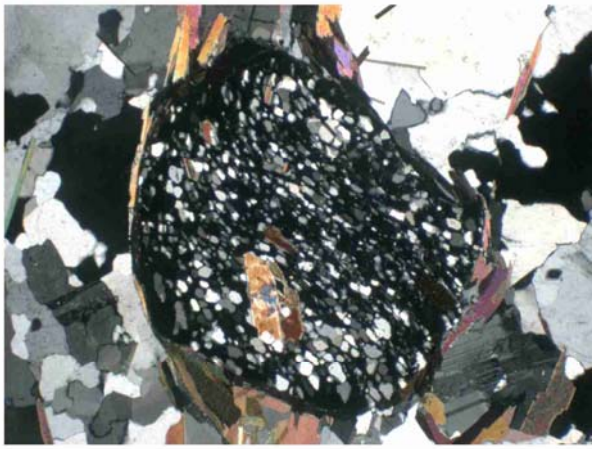

XPL- 4 mm field of view (garnet)

53- garnet mica schist

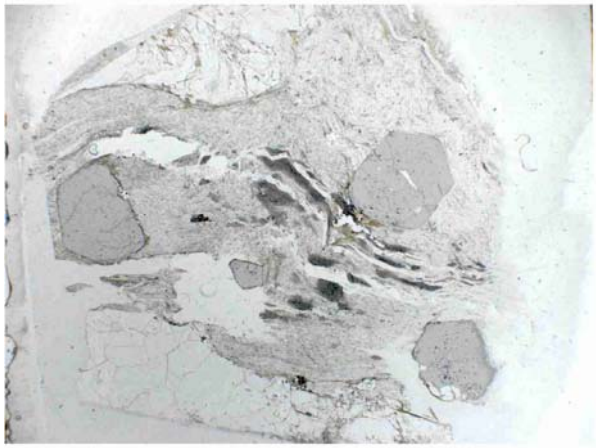

PPL- 25 mm field of view

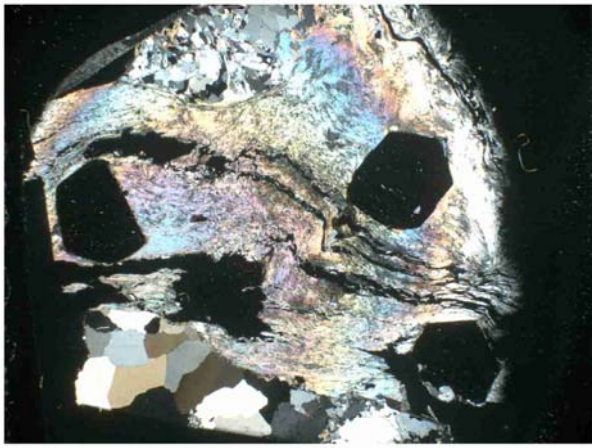

XPL- 25 mm field of view

57- garnet-fibrolite schist

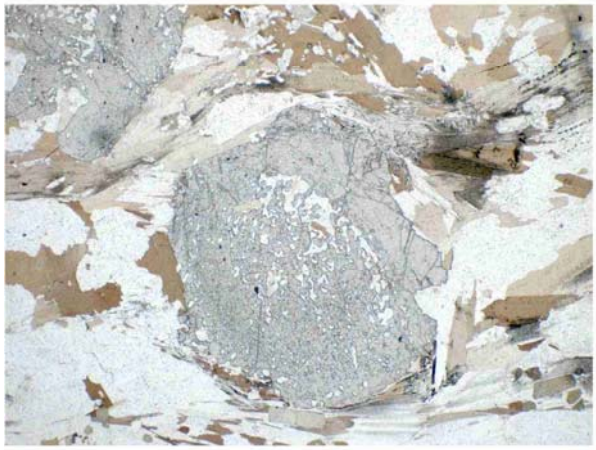

PPL- 7 mm field of view

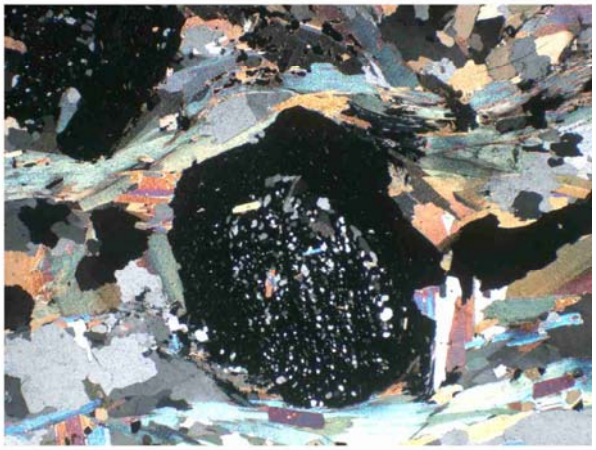

XPL- 7 mm field of view

58- orthogneiss

PPL- 28 mm field of view

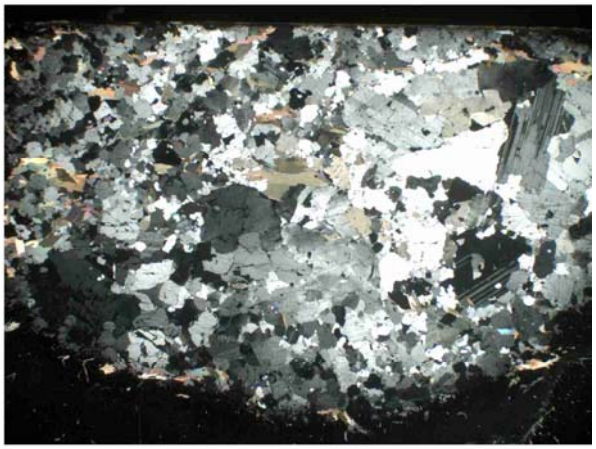

XPL- 28 mm field of view

59a- garnet-staurolite-kyanite schist

PPL- 27 mm field of view

XPL- 27 mm field of view

64a- sillimanite-mica schist

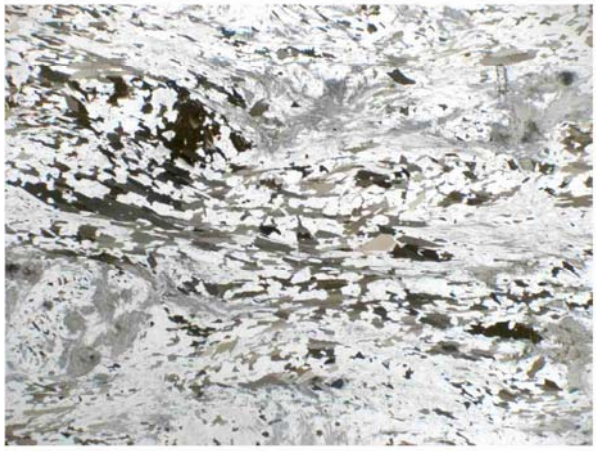

PPL- 20 mm field of view

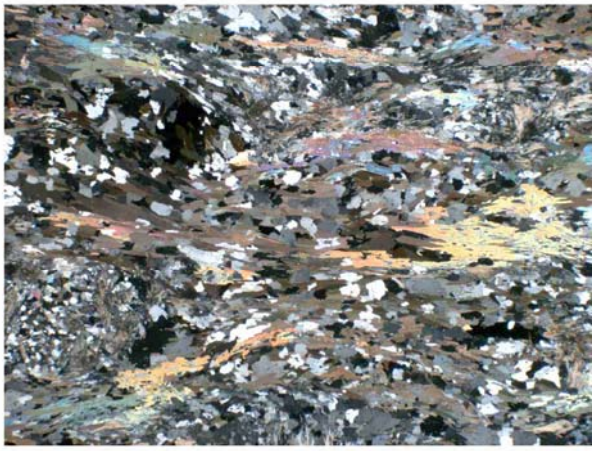

XPL- 20 mm field of view

66- garnet gneiss

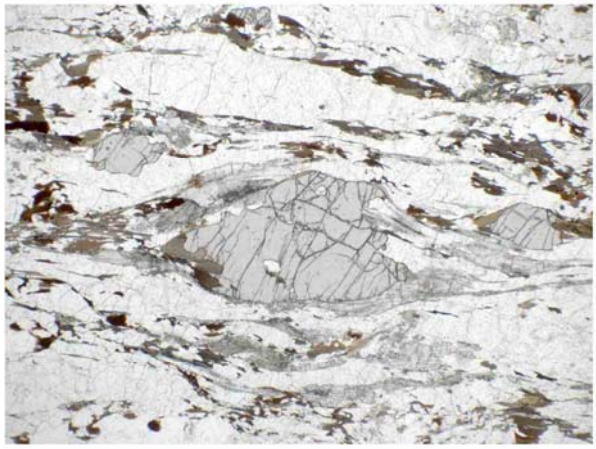

PPL- 9 mm field of view

XPL- 9 mm field of view

82- garnet-mica schist

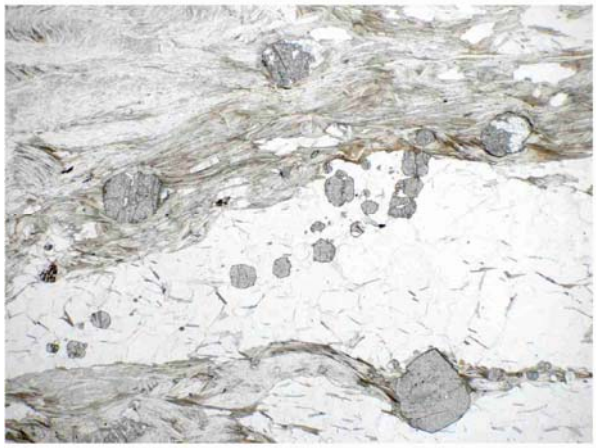

PPL- 22 mm field of view

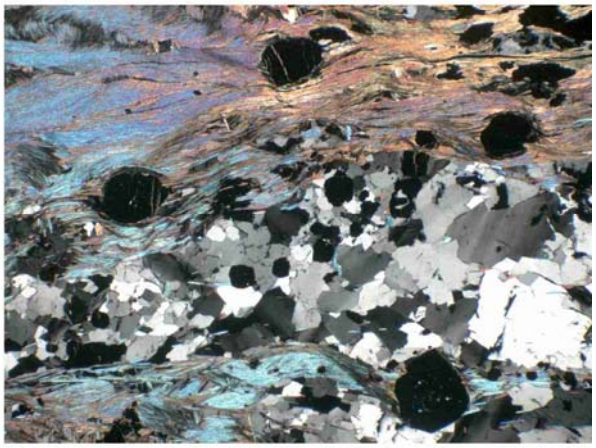

XPL- 22 mm field of view

94 garnet-mica schist

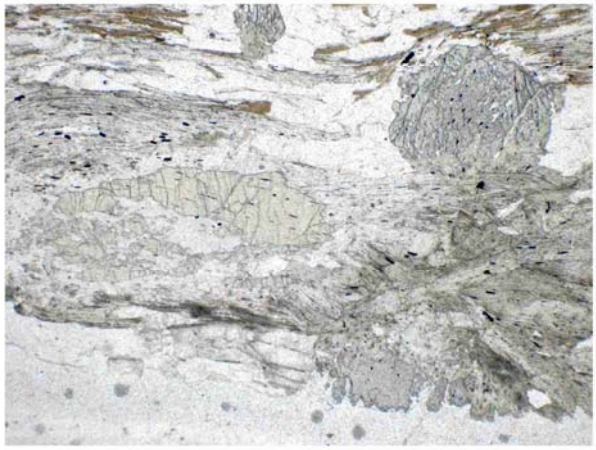

PPL- 7 mm field of view

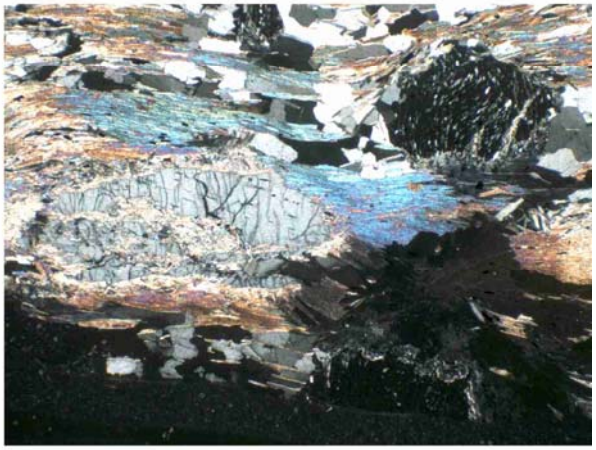

XPL- 7 mm field of view

97- mica schist

PPL- 28 mm field of view

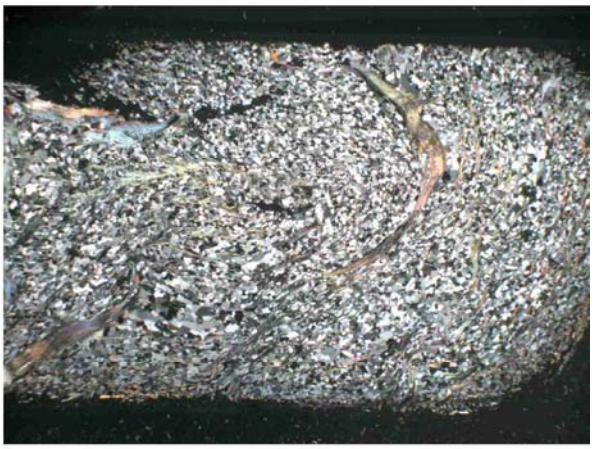

XPL- 28 mm field of view

106- garnet-mica schist

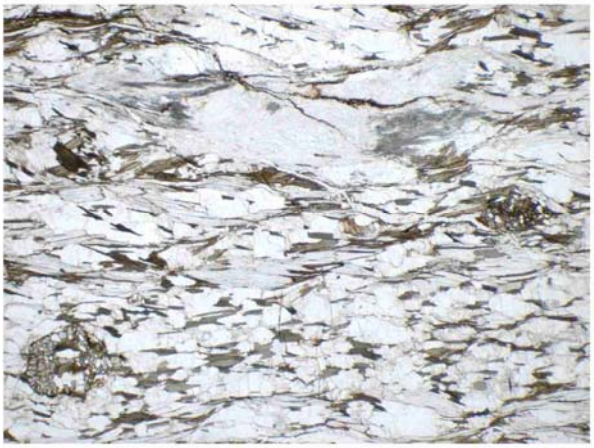

PPL- 6 mm field of view

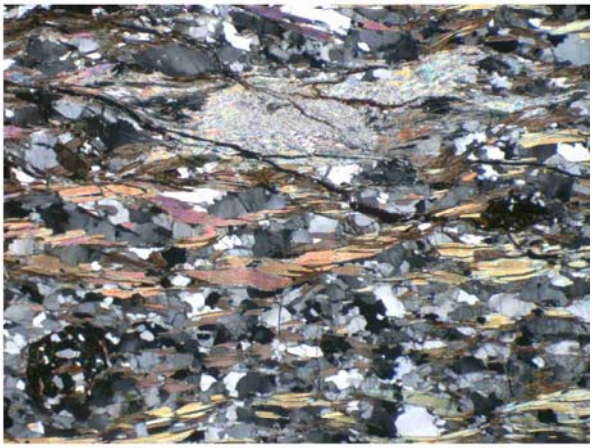

XPL- 6 mm field of view

115 orthogneiss

PPL- 28 mm field of view

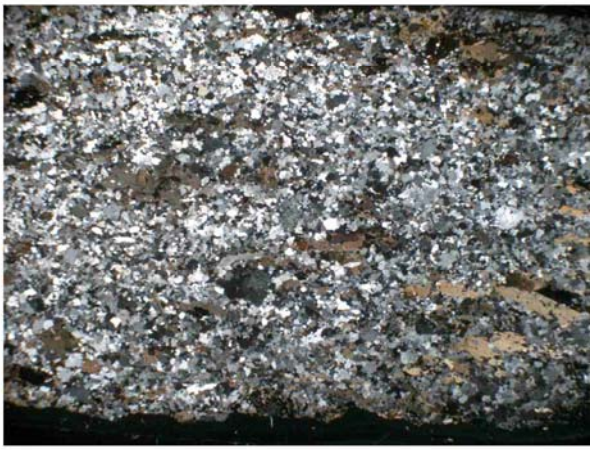

XPL- 28 mm field of view

123- fibrolite mica schist

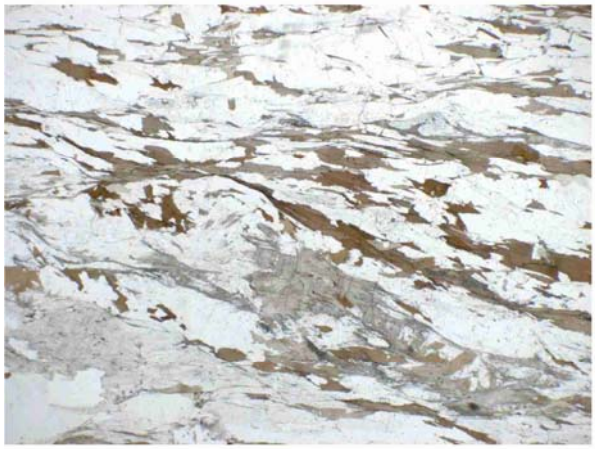

PPL- 28 mm field of view

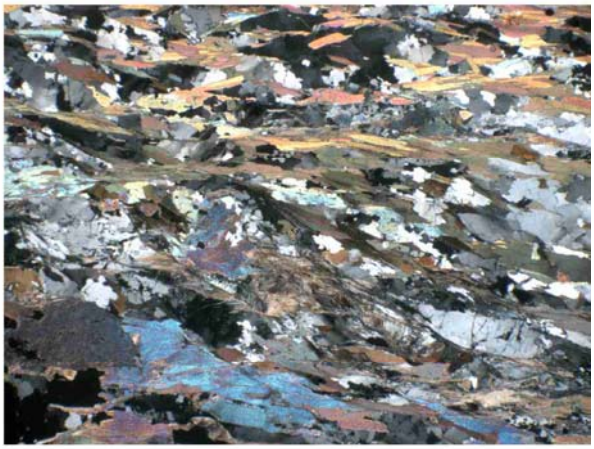

XPL- 28 mm field of view

147- kyanite-fibrolite schist

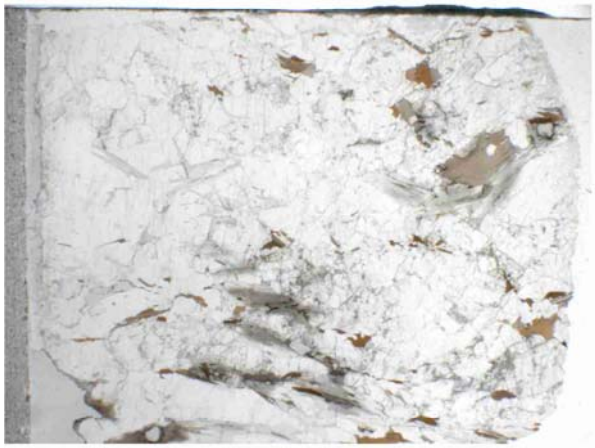

PPL- 28 mm field of view

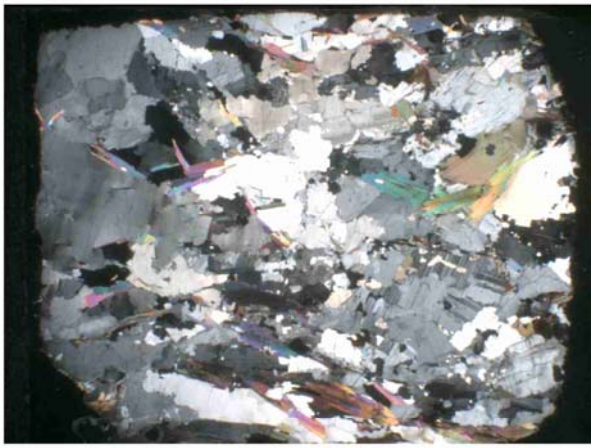

XPL- 28 mm field of view

149- chlorite-muscovite schist

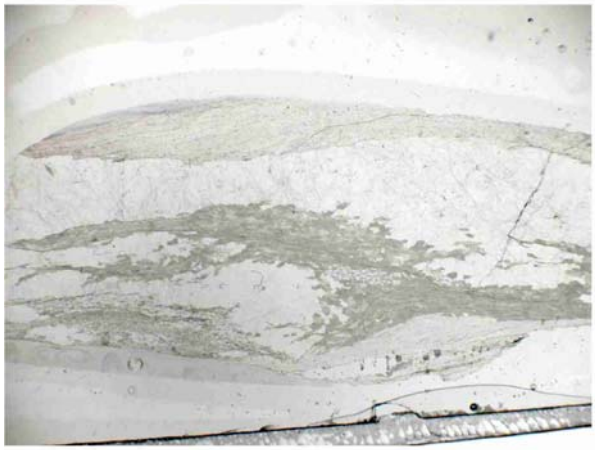

PPL- 28 mm field of view

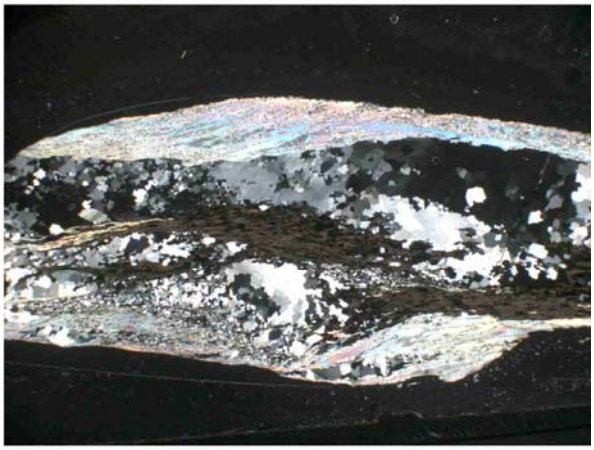

XPL- 28 mm field of view

156- garnet mica schist

PPL- 28 mm field of view

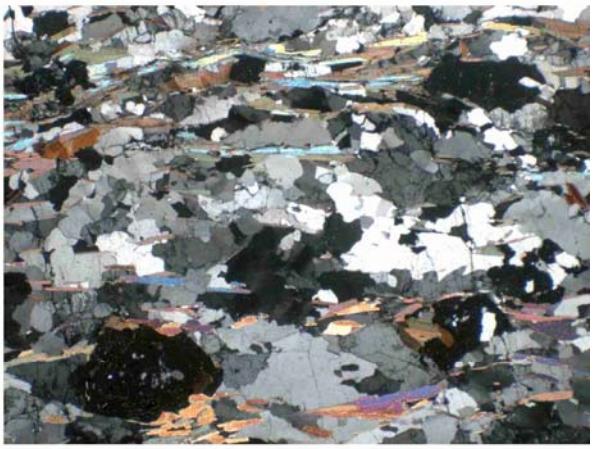

XPL- 28 mm field of view

159- fibrolite-mica schist

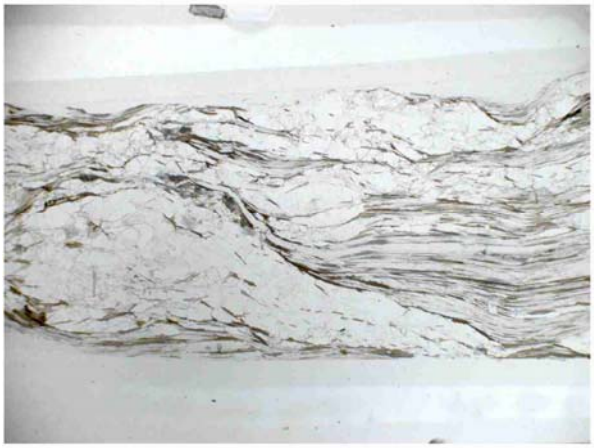

PPL- 28 mm field of view

XPL- 28 mm field of view

161- quartzite

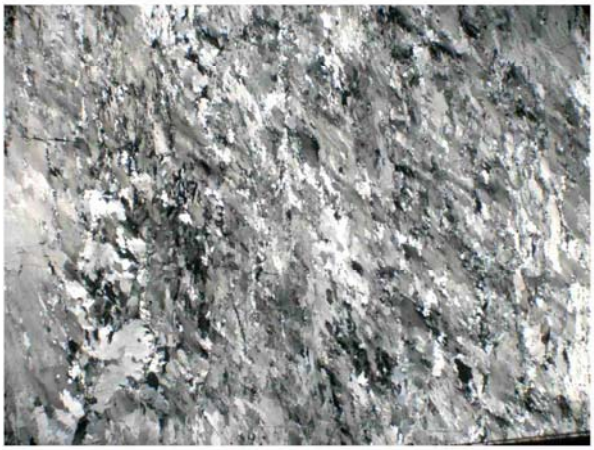

XPL- 28 mm field of view

203- quart-rich metasedimentary rock

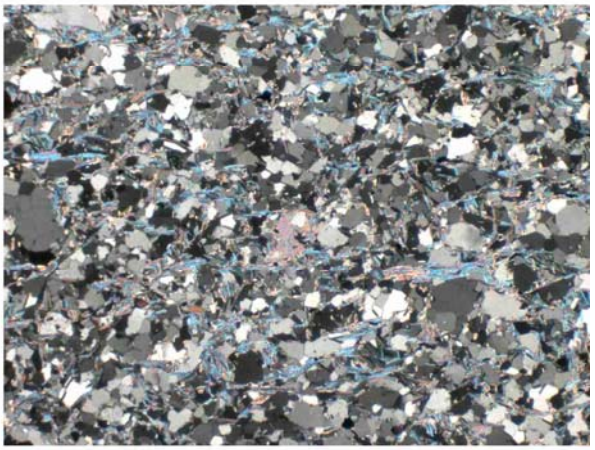

XPL- 28 mm field of view

211- quartzite

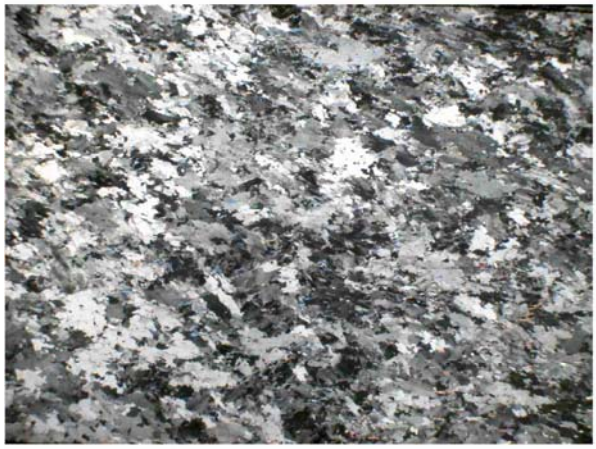

PPL- 28 mm field of view

214x- garnet-kyanite-sillimanite gneiss

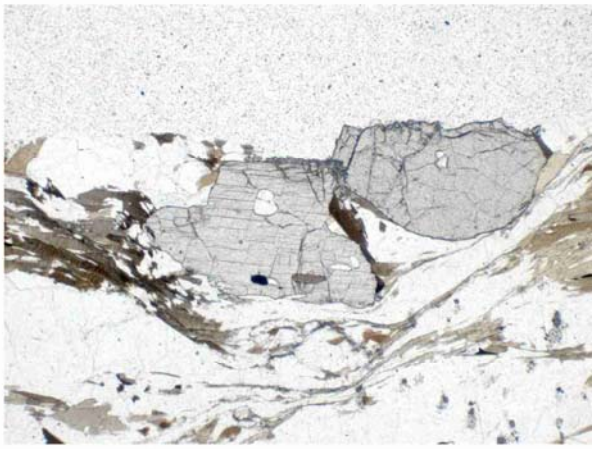

PPL- 4 mm field of view (garnet, kyanite)

214x- garnet-kyanite-sillimanite gneiss

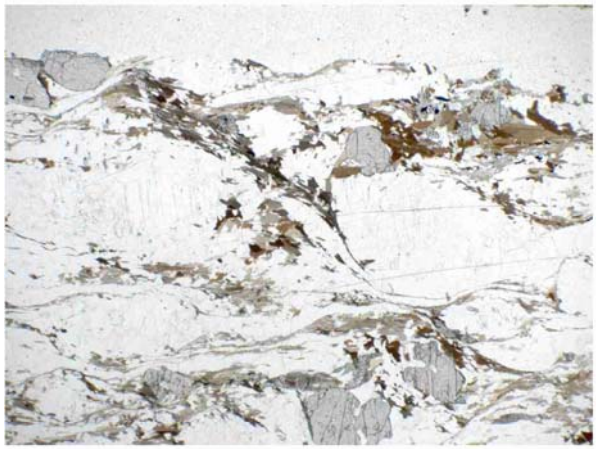

PPL- 28 mm field of view

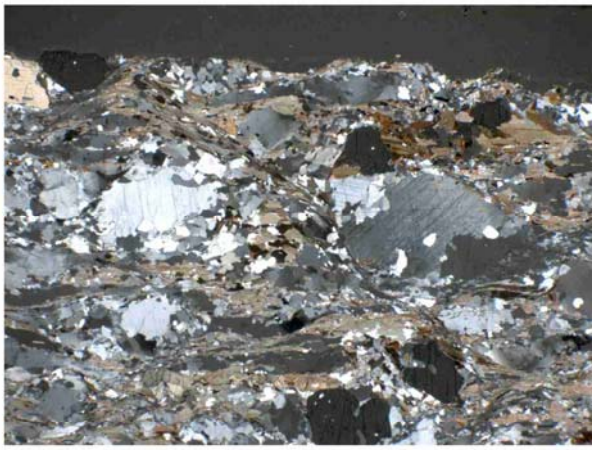

XPL- 28 mm field of view

233- orthogneiss (micaceous)

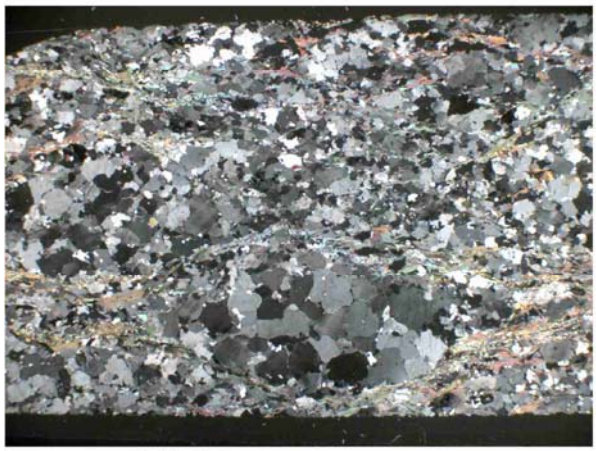

PPL- 28 mm field of view

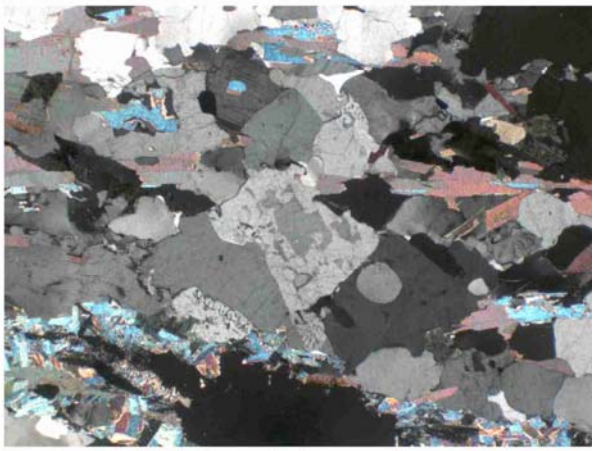

XPL- 3.5 mm field of view (melt texture)

245- orthogneiss

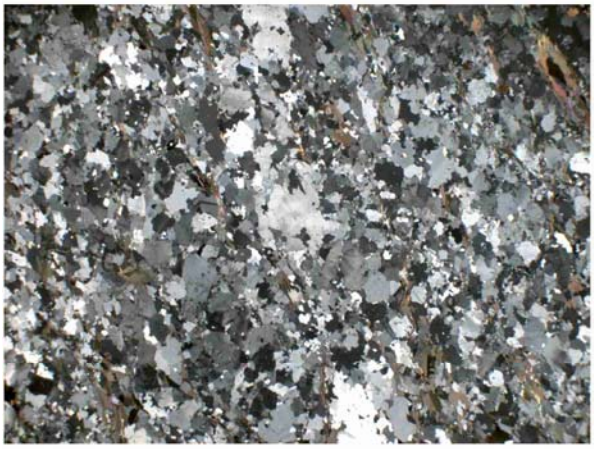

XPL- 28 mm field of view

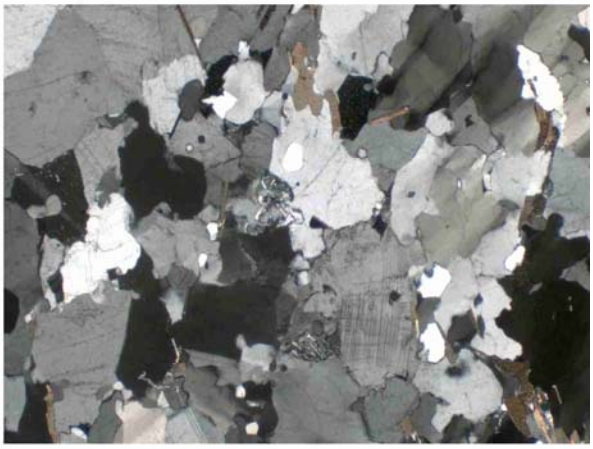

XPL- 3.5 mm field of view (melt texture)

246a- sillimanite-mica schist

PPL- 28 mm field of view

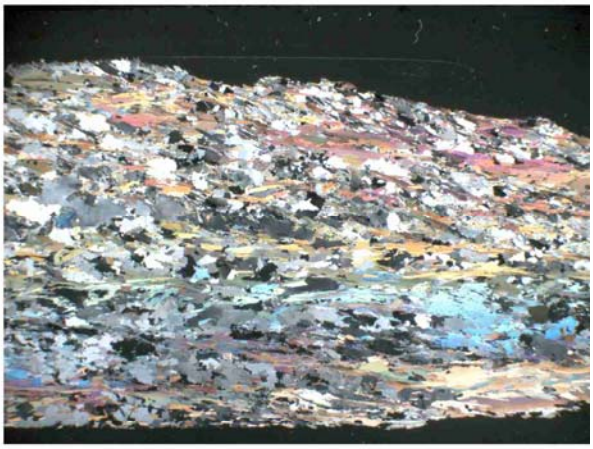

XPL- 28 mm field of view

267- garnet-sillimanite gneiss

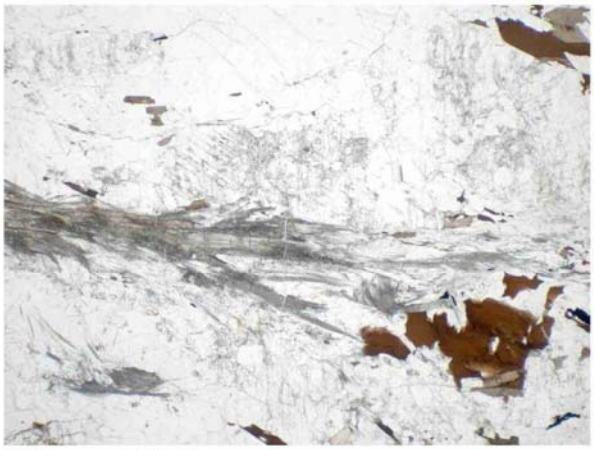

PPL- 5 mm field of view

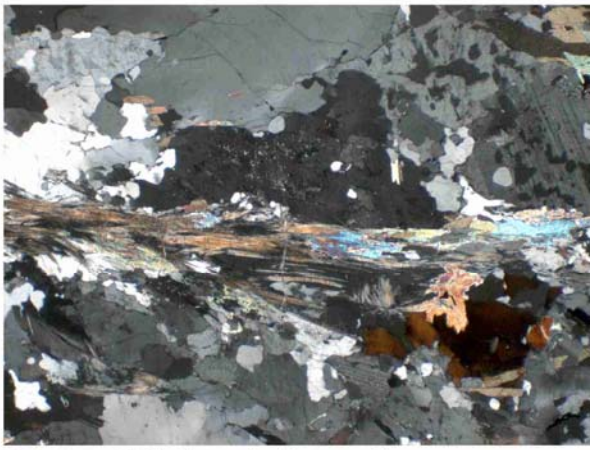

XPL- 5 mm field of view (melt texture)

275- garnet fibrolite schist

PPL- 4.5 mm field of view

XPL- 4.5 mm field of view (melt texture)

278- garnet-staurolite-kyanite schist

PPL- 28 mm field of view

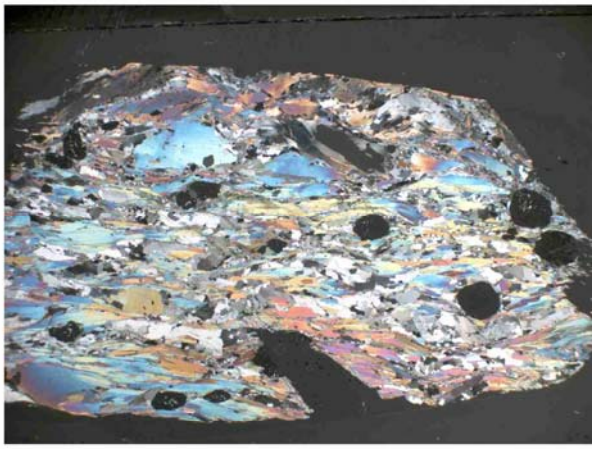

XPL- 28 mm field of view

278- key minerals

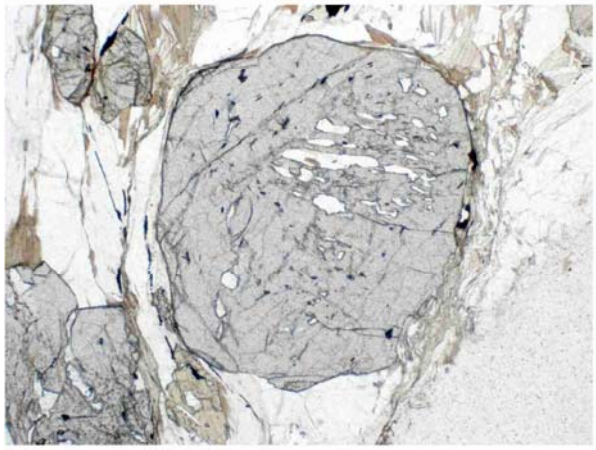

PPL- 3.5 mm field of view (garnet)

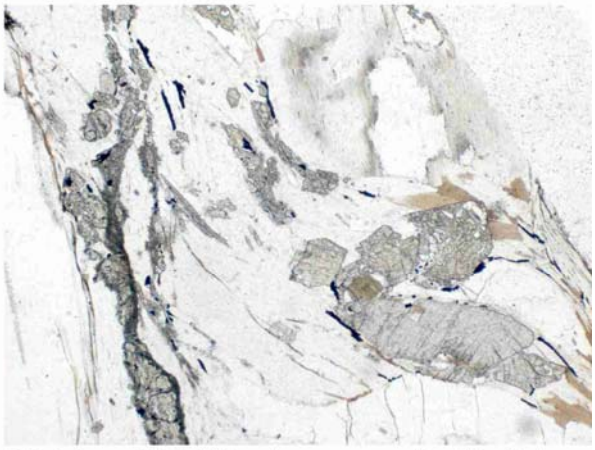

XPL- 3.5 mm field of view (garnet, staurolite, fibrolite)

280- orthogneiss

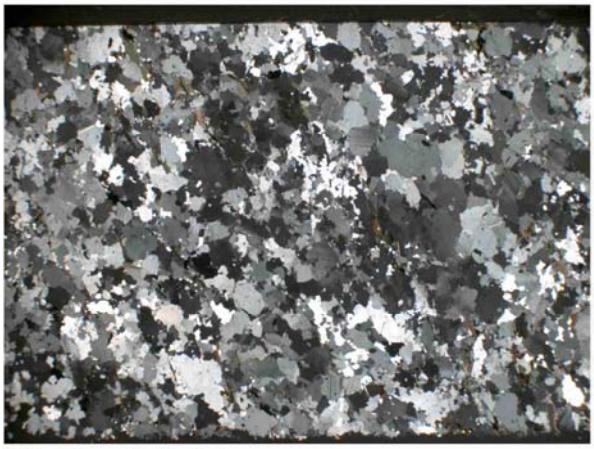

XPL- 28 mm field of view

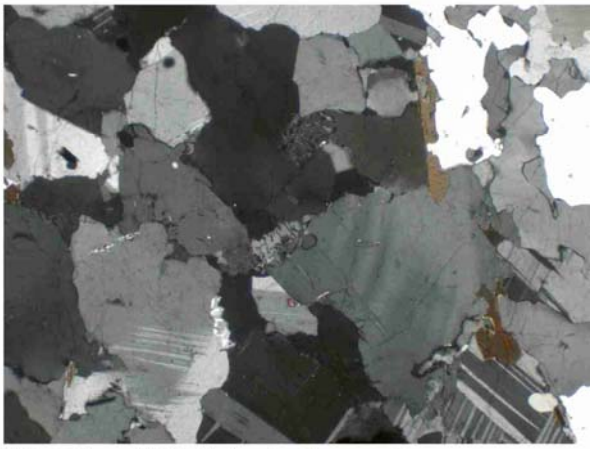

XPL- 3.5 mm field of view (melt texture)

292- quartzite (sillimanite bearing)

PPL- 28 mm field of view

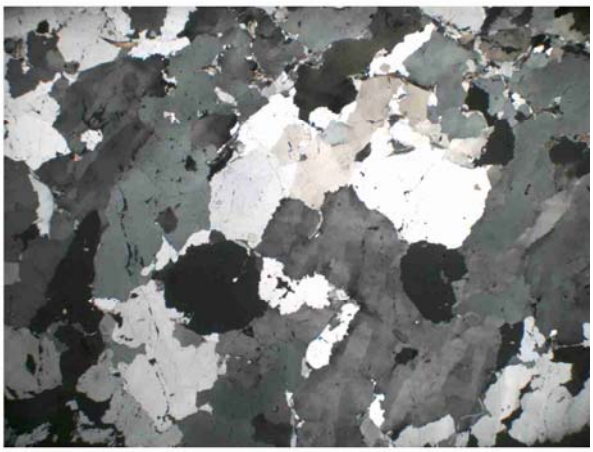

XPL- 8 mm field of view (close up)

Photomicrographs of all samples analysed for geochronology (detrital zircon and orthogneiss) and Nd geochemistry. Full sample descriptions and locations can be found in sample table x. PPL= Plane polarized light, XPL= cross polarised light.

S3. Atlas of zircon Cathodoluminescence images

A representative se**le**ction of zircons from each detrital zircon/ orthogenesis sample analysed. All ages $^{207}Pb/^{206}Pb$ ages **(**± 2σ abs). See appendix A5 zircon data table for full data set.

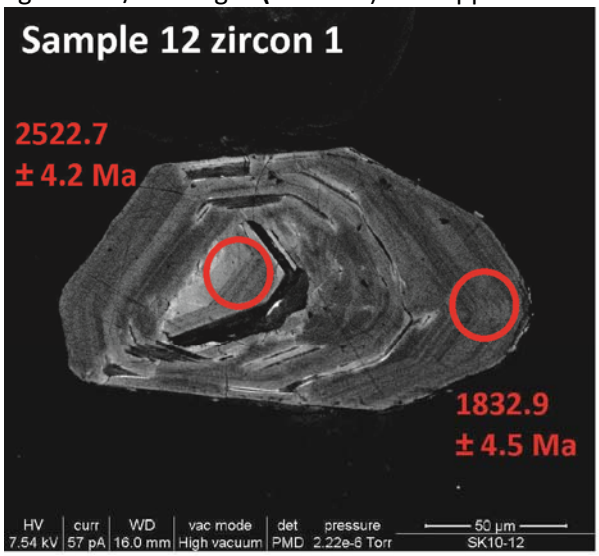

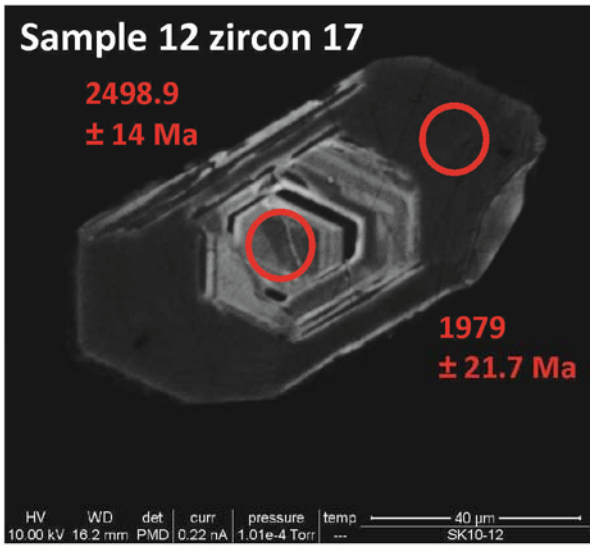

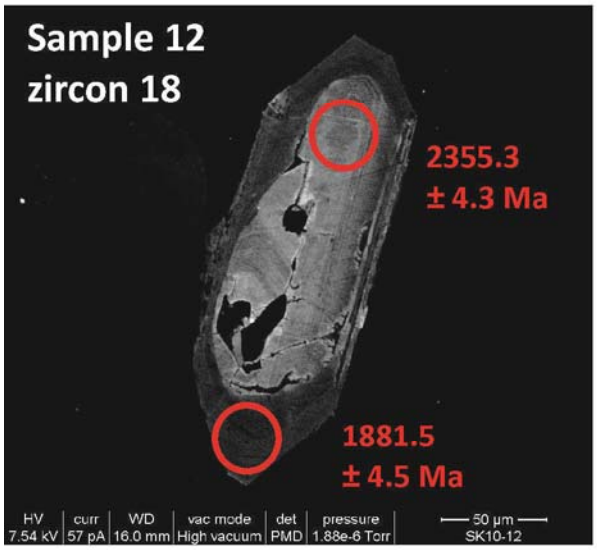

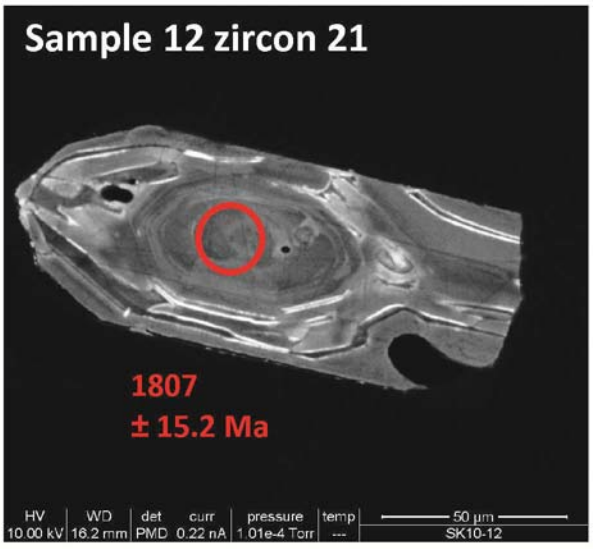

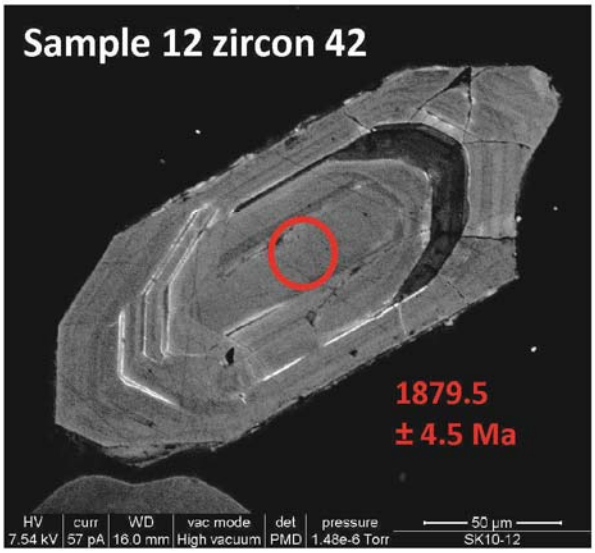

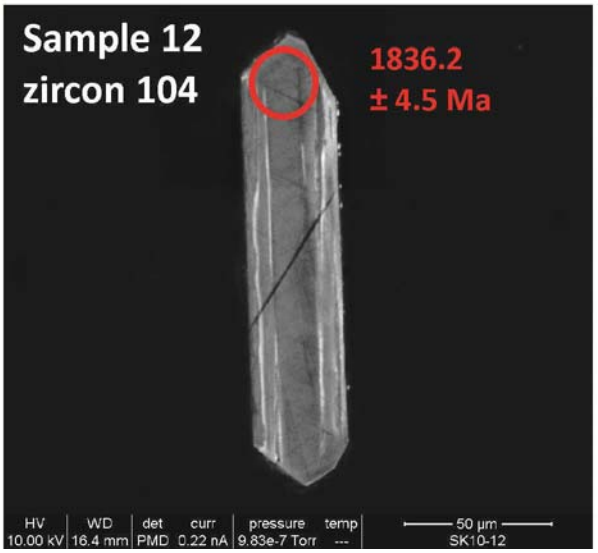


Sample 32 zircon 4L
830.1
± 5.7 Ma
HV curr det vacMode WD 100 µm
10.00 kV 3.6 nA PMD High vacuum 16.3 mm SK12-32


Sample 32 zircon 1M
856
± 7.9 Ma
1851.8
± 4.5 Ma
HV curr det vacMode WD 50 µm
10.00 kV 3.6 nA PMD High vacuum 16.3 mm SK12-32

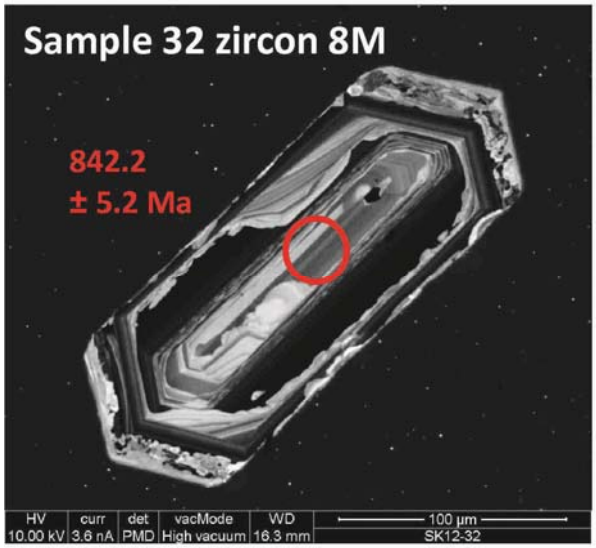
Sample 32 zircon 8M
842.2
± 5.2 Ma
HV curr det vacMode WD 100 µm
10.00 kV 3.6 nA PMD High vacuum 16.3 mm SK12-32

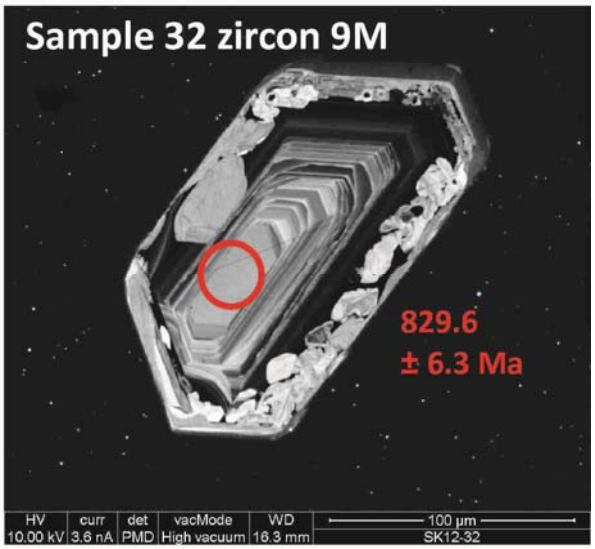
Sample 32 zircon 9M
829.6
± 6.3 Ma
HV curr det vacMode WD 100 µm
10.00 kV 3.6 nA PMD High vacuum 16.3 mm SK12-32

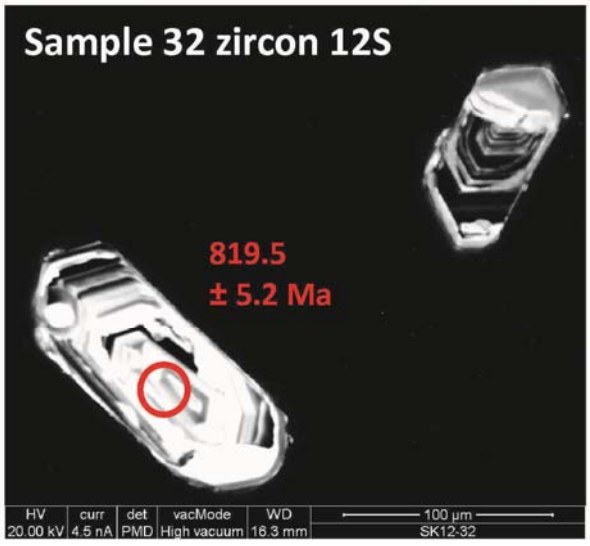
Sample 32 zircon 12S
819.5
± 5.2 Ma
HV curr det vacMode WD 100 µm
20.00 kV 4.5 nA PMD High vacuum 16.3 mm SK12-32

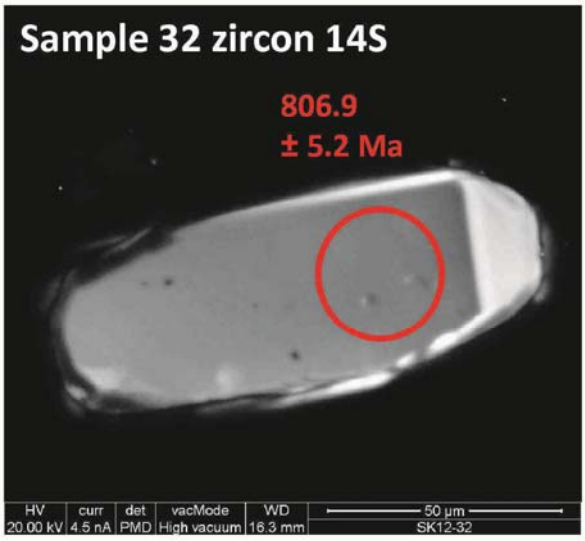
Sample 32 zircon 14S
806.9
± 5.2 Ma
HV curr det vacMode WD 50 µm
20.00 kV 4.5 nA PMD High vacuum 16.3 mm SK12-32

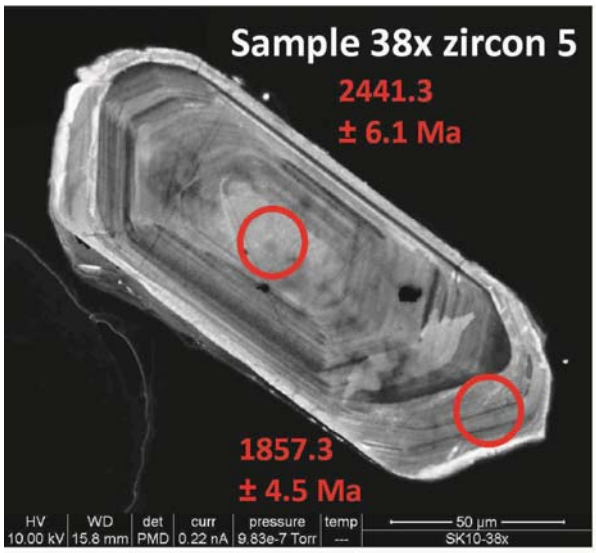
Sample 38x zircon 5
2441.3
± 6.1 Ma
1857.3
± 4.5 Ma
HV 10.00 kV | WD 15.8 mm | det PMD | curr 0.22 nA | pressure 9.83e-7 Torr | temp --- | 50 µm SK10-38x

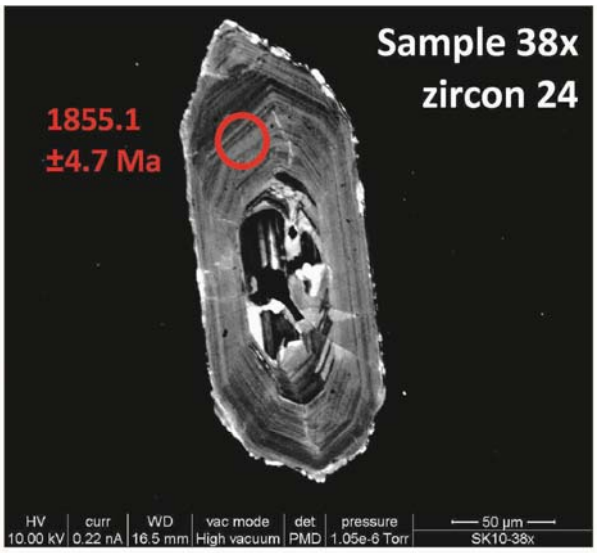
Sample 38x zircon 24
1855.1
±4.7 Ma
HV 10.00 kV | curr 0.22 nA | WD 16.5 mm | vac mode High vacuum | det PMD | pressure 1.05e-6 Torr | 50 µm SK10-38x


Sample 38x zircon 37
1843.1
± 4.5 Ma
HV 10.00 kV | WD 15.8 mm | det PMD | curr 0.22 nA | pressure 7.77e-7 Torr | temp --- | 50 µm SK10-38x

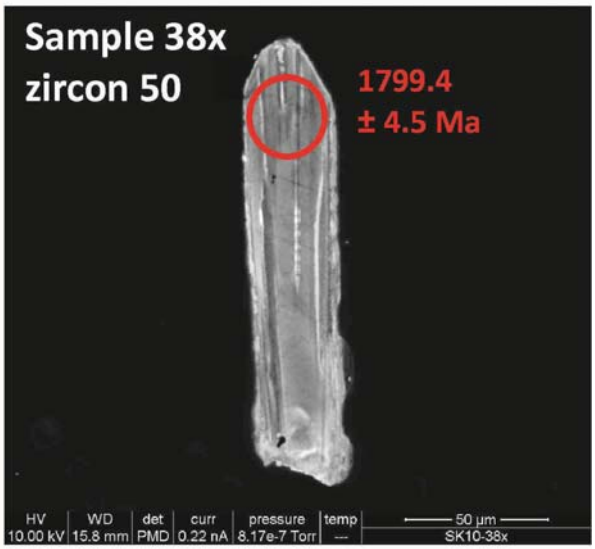
Sample 38x zircon 50
1799.4
± 4.5 Ma
HV 10.00 kV | WD 15.8 mm | det PMD | curr 0.22 nA | pressure 8.17e-7 Torr | temp --- | 50 µm SK10-38x

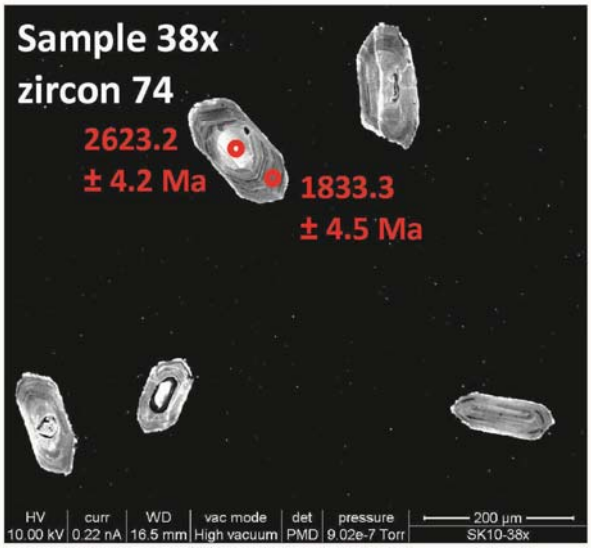
Sample 38x zircon 74
2623.2
± 4.2 Ma
1833.3
± 4.5 Ma
HV 10.00 kV | curr 0.22 nA | WD 16.5 mm | vac mode High vacuum | det PMD | pressure 9.02e-7 Torr | 200 µm SK10-38x

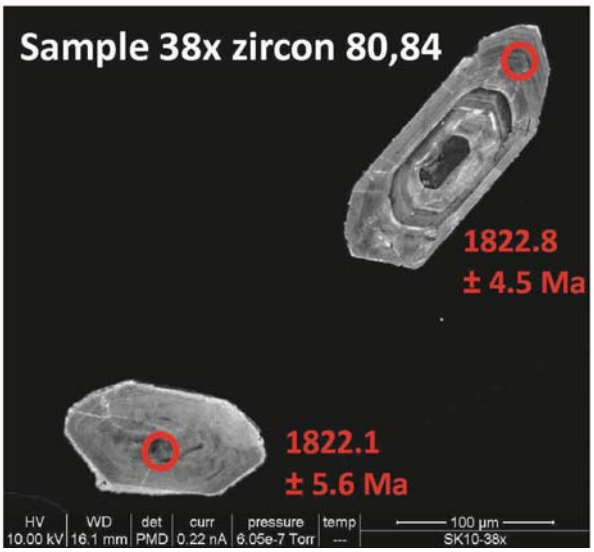
Sample 38x zircon 80,84
1822.8
± 4.5 Ma
1822.1
± 5.6 Ma
HV 10.00 kV | WD 16.1 mm | det PMD | curr 0.22 nA | pressure 6.05e-7 Torr | temp --- | 100 µm SK10-38x

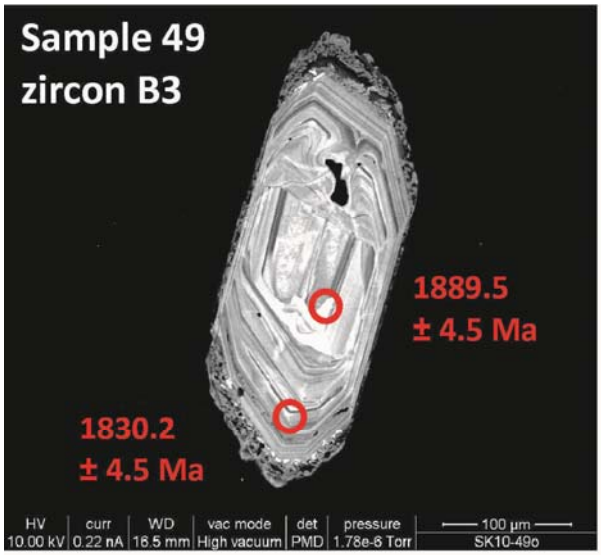
Sample 49
zircon B3
1889.5
± 4.5 Ma
1830.2
± 4.5 Ma
HV curr WD vac mode det pressure 100 µm
10.00 kV 0.22 nA 16.5 mm High vacuum PMD 1.78e-6 Torr SK10-49o

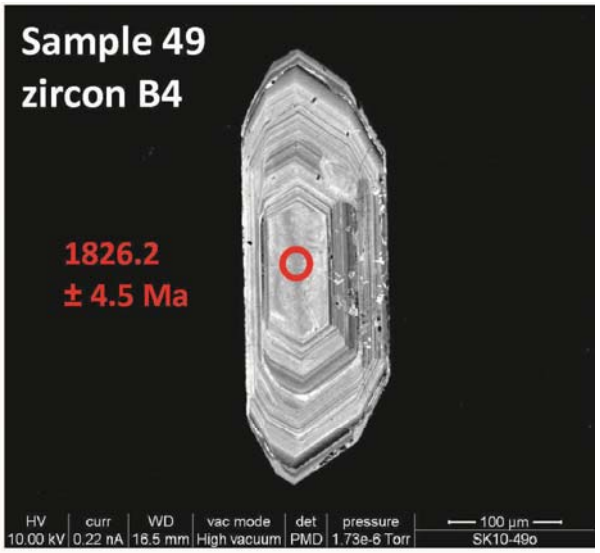
Sample 49
zircon B4
1826.2
± 4.5 Ma
HV curr WD vac mode det pressure 100 µm
10.00 kV 0.22 nA 16.5 mm High vacuum PMD 1.73e-6 Torr SK10-49o

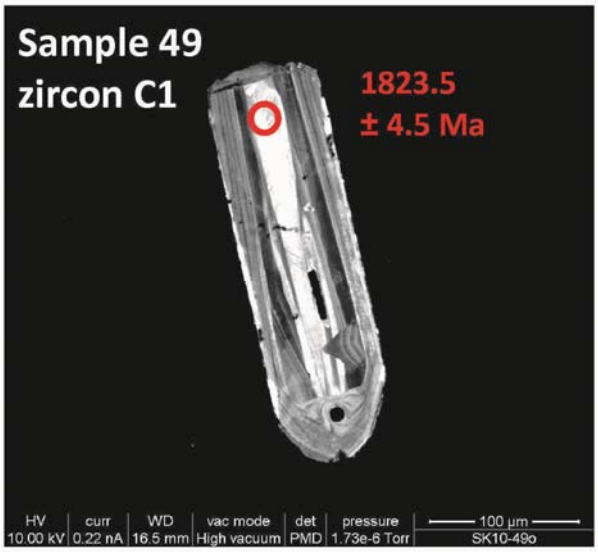
Sample 49
zircon C1
1823.5
± 4.5 Ma
HV curr WD vac mode det pressure 100 µm
10.00 kV 0.22 nA 16.5 mm High vacuum PMD 1.73e-6 Torr SK10-49o

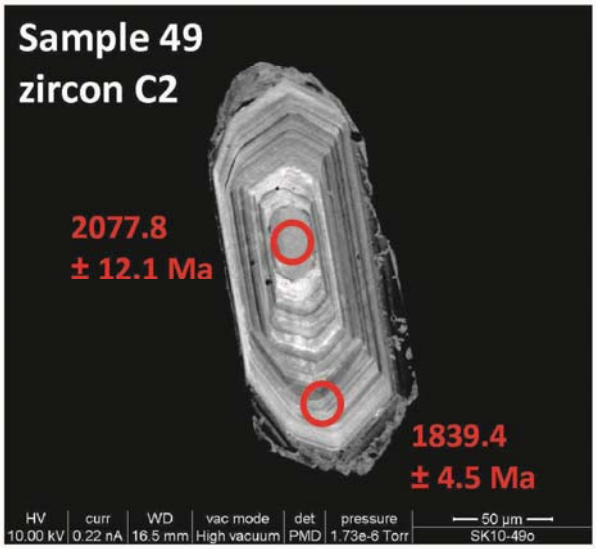
Sample 49
zircon C2
2077.8
± 12.1 Ma
1839.4
± 4.5 Ma
HV curr WD vac mode det pressure 50 µm
10.00 kV 0.22 nA 16.5 mm High vacuum PMD 1.73e-6 Torr SK10-49o

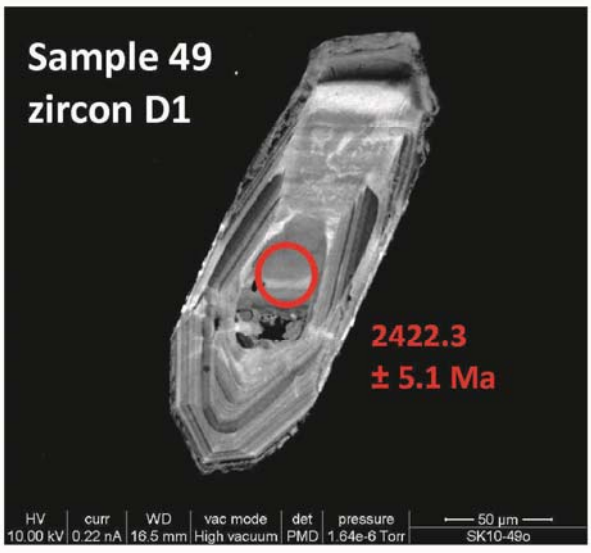
Sample 49
zircon D1
2422.3
± 5.1 Ma
HV curr WD vac mode det pressure 50 µm
10.00 kV 0.22 nA 16.5 mm High vacuum PMD 1.64e-6 Torr SK10-49o

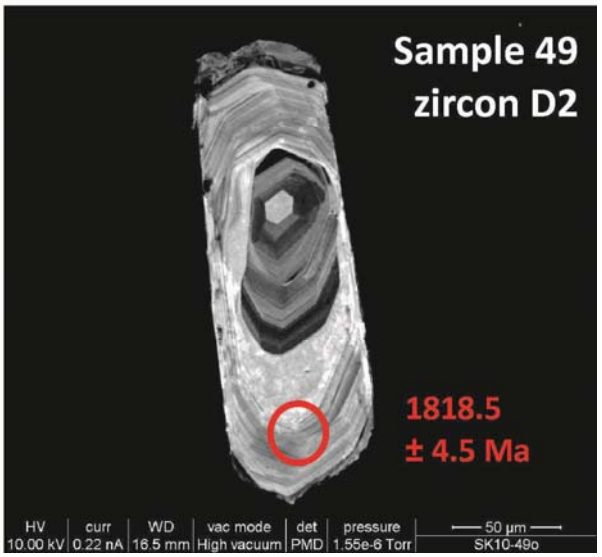
Sample 49
zircon D2
1818.5
± 4.5 Ma
HV curr WD vac mode det pressure 50 µm
10.00 kV 0.22 nA 16.5 mm High vacuum PMD 1.55e-6 Torr SK10-49o

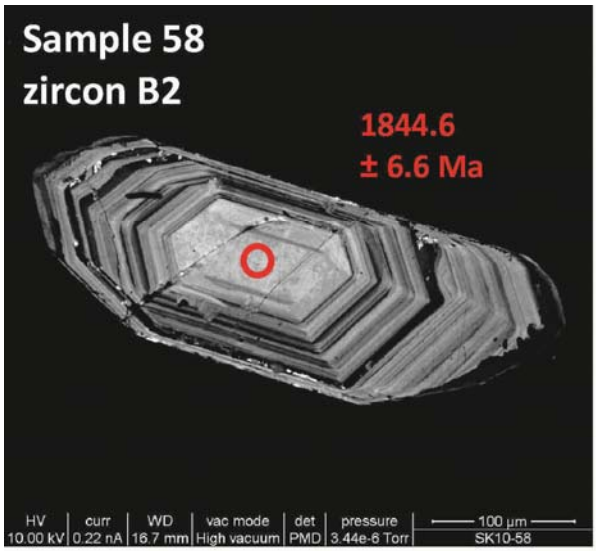
Sample 58
zircon B2
1844.6
± 6.6 Ma
HV 10.00 kV | curr 0.22 nA | WD 16.7 mm | vac mode High vacuum | det PMD | pressure 3.44e-6 Torr | 100 µm | SK10-58

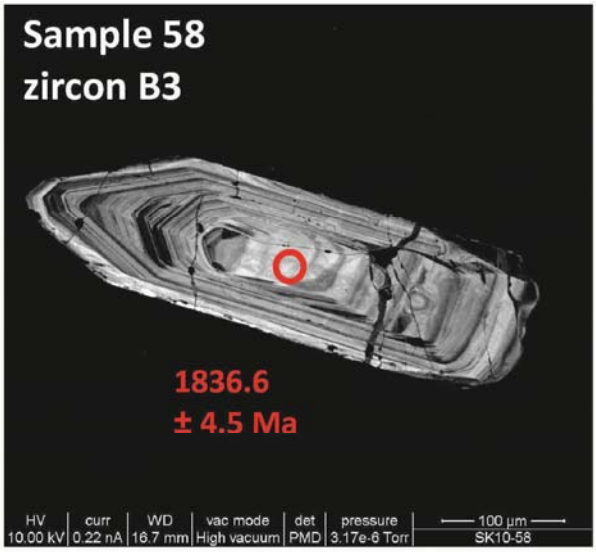
Sample 58
zircon B3
1836.6
± 4.5 Ma
HV 10.00 kV | curr 0.22 nA | WD 16.7 mm | vac mode High vacuum | det PMD | pressure 3.17e-6 Torr | 100 µm | SK10-58

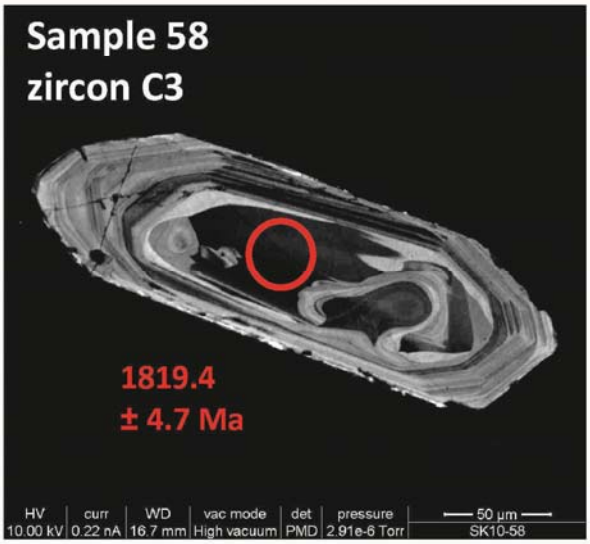
Sample 58
zircon C3
1819.4
± 4.7 Ma
HV 10.00 kV | curr 0.22 nA | WD 16.7 mm | vac mode High vacuum | det PMD | pressure 2.91e-6 Torr | 50 µm | SK10-58

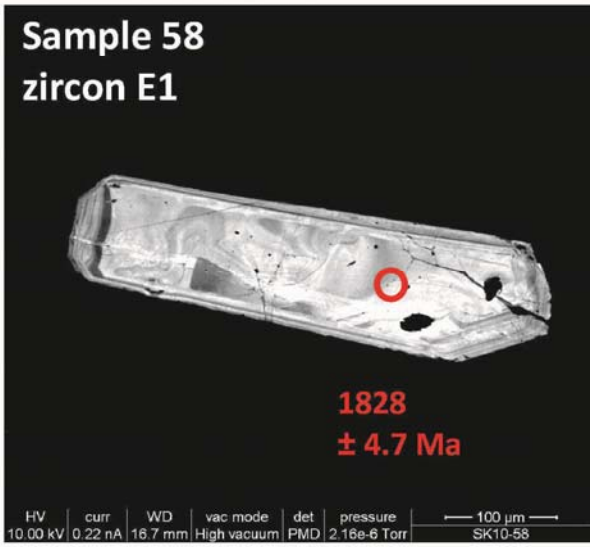
Sample 58
zircon E1
1828
± 4.7 Ma
HV 10.00 kV | curr 0.22 nA | WD 16.7 mm | vac mode High vacuum | det PMD | pressure 2.16e-6 Torr | 100 µm | SK10-58


Sample 58
zircon E2
1823
± 4.5 Ma
HV 10.00 kV | curr 0.22 nA | WD 16.7 mm | vac mode High vacuum | det PMD | pressure 2.16e-6 Torr | 50 µm | SK10-58

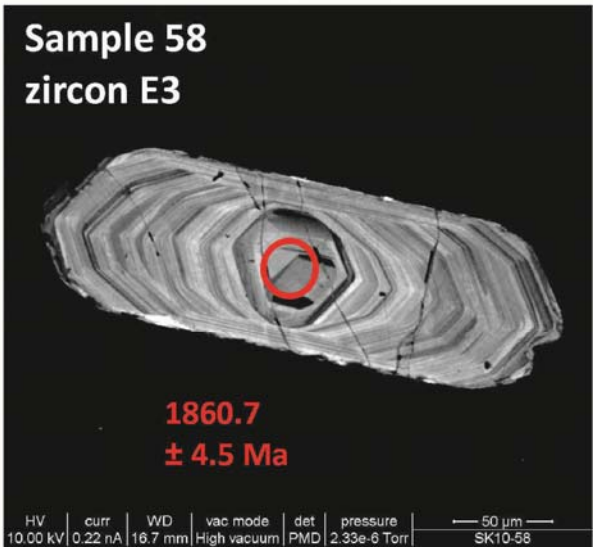
Sample 58
zircon E3
1860.7
± 4.5 Ma
HV 10.00 kV | curr 0.22 nA | WD 16.7 mm | vac mode High vacuum | det PMD | pressure 2.33e-6 Torr | 50 µm | SK10-58

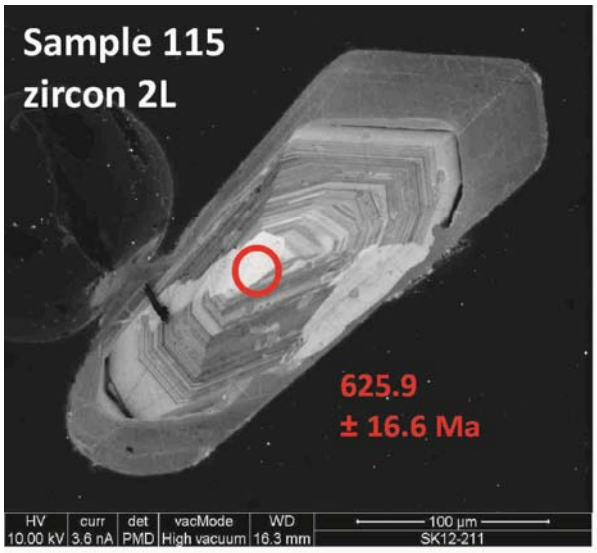
Sample 115
zircon 2L
625.9
± 16.6 Ma
HV 10.00 kV | curr 3.6 nA | det PMD | vacMode High vacuum | WD 16.3 mm | 100 µm | SK12-211

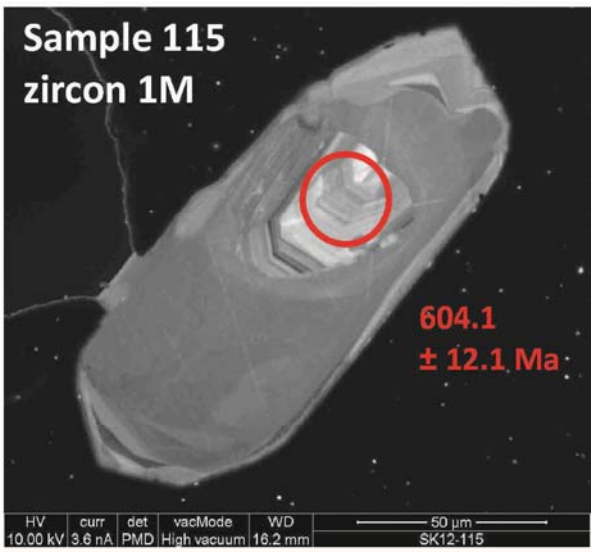
Sample 115
zircon 1M
604.1
± 12.1 Ma
HV 10.00 kV | curr 3.6 nA | det PMD | vacMode High vacuum | WD 16.2 mm | 50 µm | SK12-115

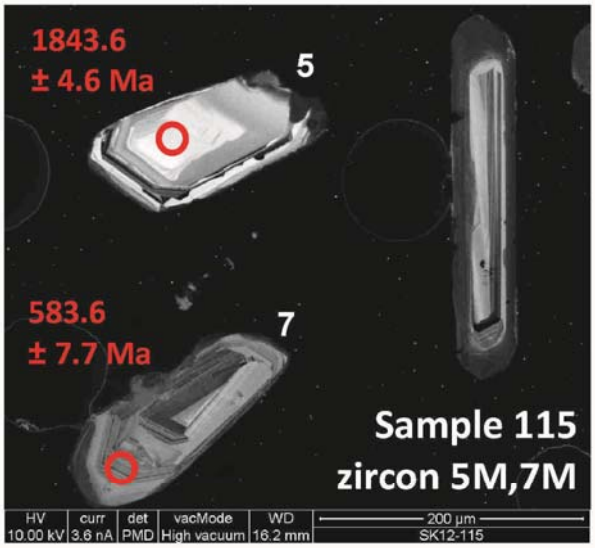
1843.6
± 4.6 Ma
5
583.6
± 7.7 Ma
7
Sample 115
zircon 5M,7M
HV 10.00 kV | curr 3.6 nA | det PMD | vacMode High vacuum | WD 16.2 mm | 200 µm | SK12-115

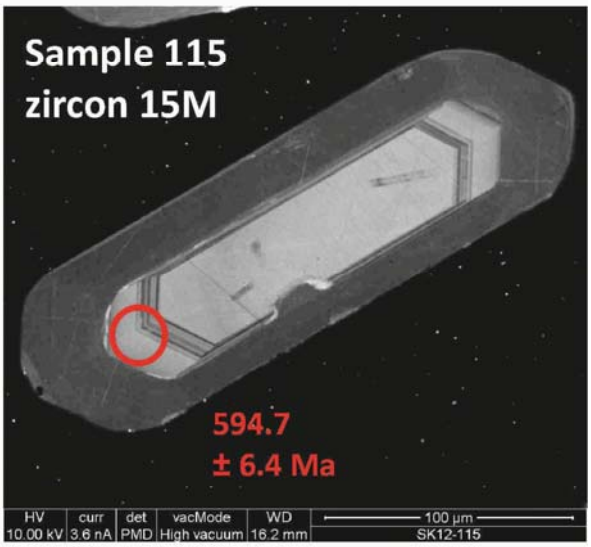
Sample 115
zircon 15M
594.7
± 6.4 Ma
HV 10.00 kV | curr 3.6 nA | det PMD | vacMode High vacuum | WD 16.2 mm | 100 µm | SK12-115

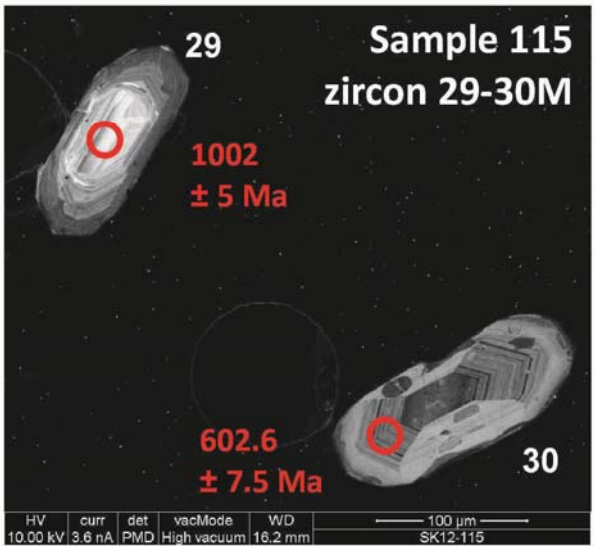
29
Sample 115
zircon 29-30M
1002
± 5 Ma
602.6
± 7.5 Ma
30
HV 10.00 kV | curr 3.6 nA | det PMD | vacMode High vacuum | WD 16.2 mm | 100 µm | SK12-115

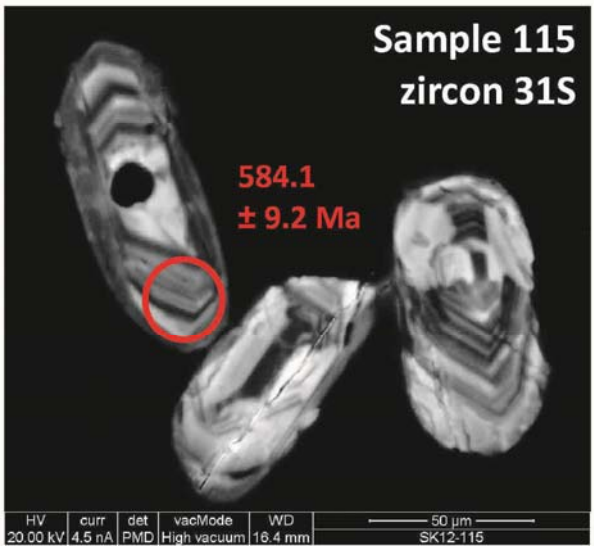
Sample 115
zircon 31S
584.1
± 9.2 Ma
HV 20.00 kV | curr 4.5 nA | det PMD | vacMode High vacuum | WD 16.4 mm | 50 µm | SK12-115

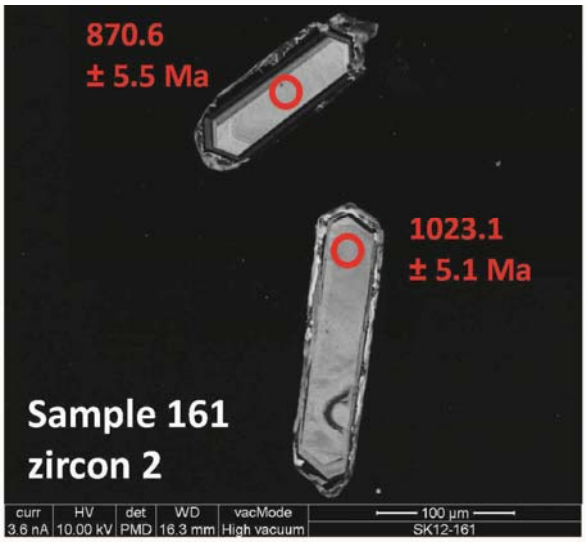
870.6
± 5.5 Ma
1023.1
± 5.1 Ma
Sample 161
zircon 2
curr 3.6 nA
HV 10.00 kV
det PMD
WD 16.3 mm
vacMode High vacuum
100 µm
SK12-161

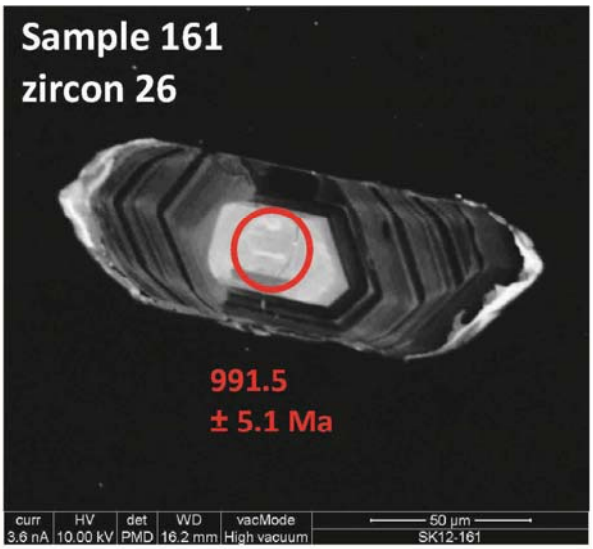
Sample 161
zircon 26
991.5
± 5.1 Ma
curr 3.6 nA
HV 10.00 kV
det PMD
WD 16.2 mm
vacMode High vacuum
50 µm
SK12-161

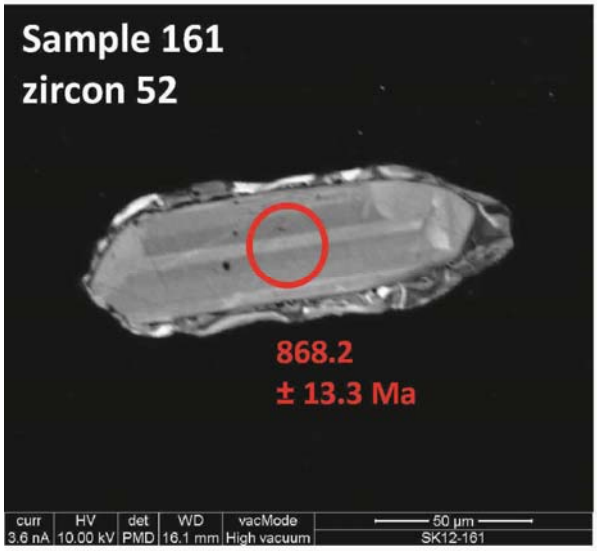
Sample 161
zircon 52
868.2
± 13.3 Ma
curr 3.6 nA
HV 10.00 kV
det PMD
WD 16.1 mm
vacMode High vacuum
50 µm
SK12-161

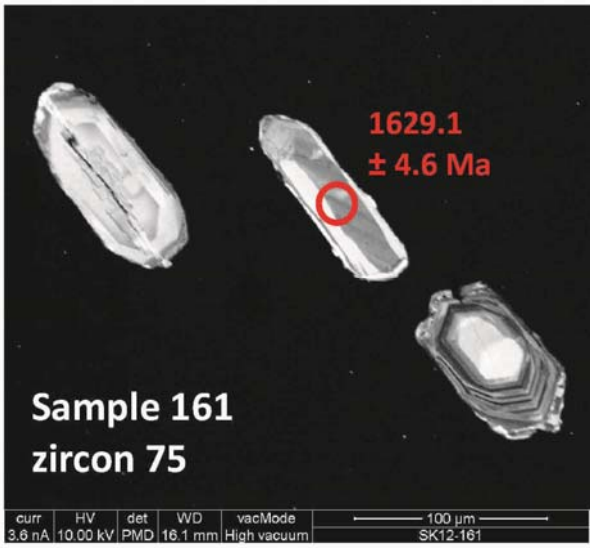
1629.1
± 4.6 Ma
Sample 161
zircon 75
curr 3.6 nA
HV 10.00 kV
det PMD
WD 16.1 mm
vacMode High vacuum
100 µm
SK12-161

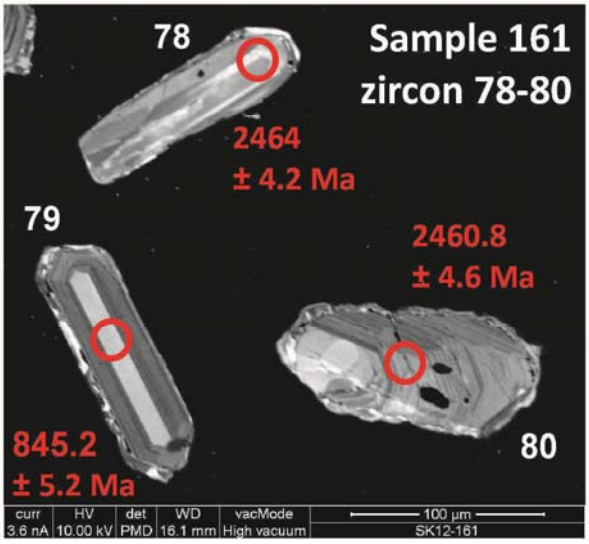
78
Sample 161
zircon 78-80
2464
± 4.2 Ma
79
2460.8
± 4.6 Ma
845.2
± 5.2 Ma
80
curr 3.6 nA
HV 10.00 kV
det PMD
WD 16.1 mm
vacMode High vacuum
100 µm
SK12-161

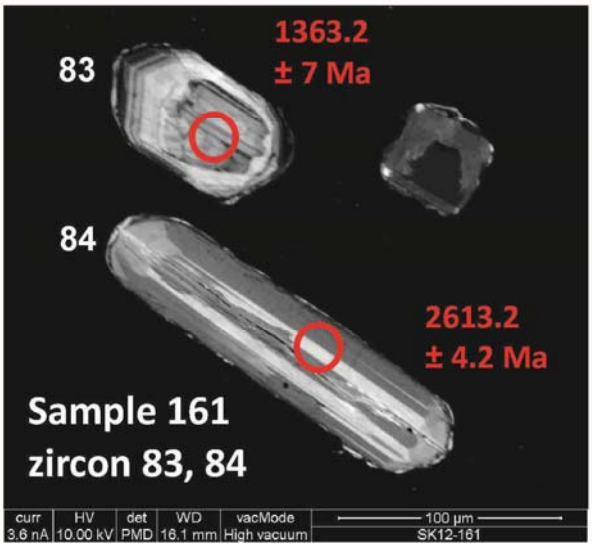
83
1363.2
± 7 Ma
84
2613.2
± 4.2 Ma
Sample 161
zircon 83, 84
curr 3.6 nA
HV 10.00 kV
det PMD
WD 16.1 mm
vacMode High vacuum
100 µm
SK12-161

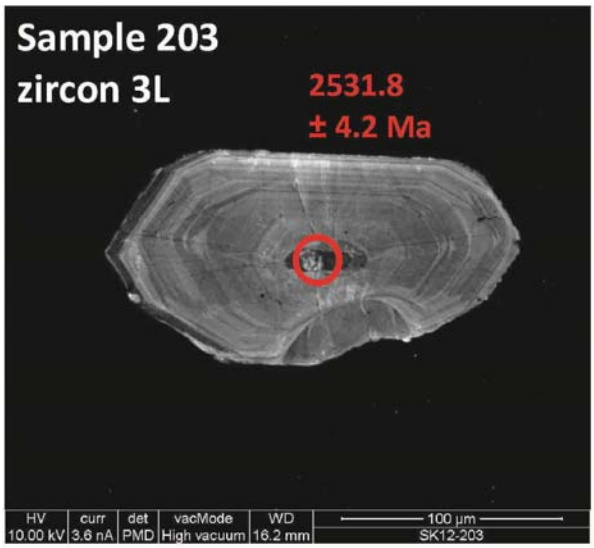
Sample 203
zircon 3L
2531.8
± 4.2 Ma
HV 10.00 kV | curr 3.6 nA | det PMD | vacMode High vacuum | WD 16.2 mm | 100 µm | SK12-203

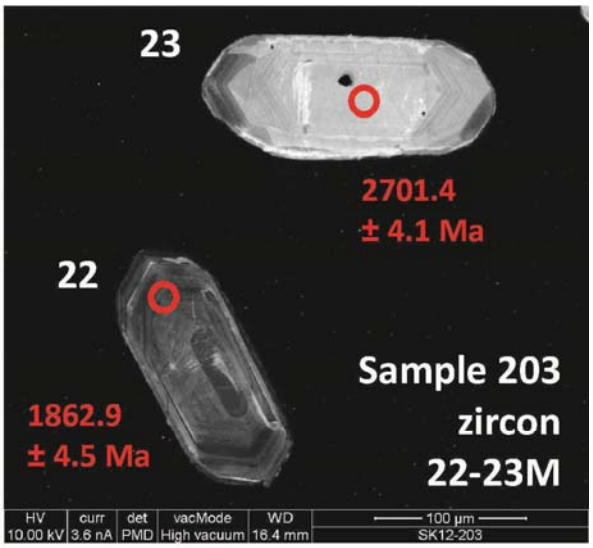
23
2701.4
± 4.1 Ma
22
1862.9
± 4.5 Ma
Sample 203
zircon
22-23M
HV 10.00 kV | curr 3.6 nA | det PMD | vacMode High vacuum | WD 16.4 mm | 100 µm | SK12-203

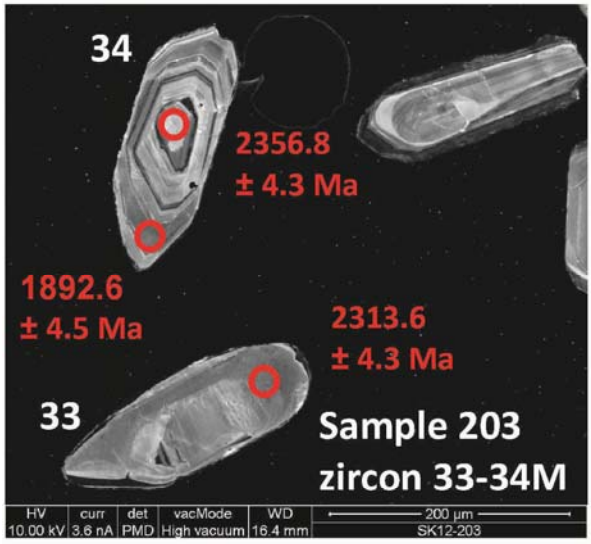
34
2356.8
± 4.3 Ma
1892.6
± 4.5 Ma
2313.6
± 4.3 Ma
33
Sample 203
zircon 33-34M
HV 10.00 kV | curr 3.6 nA | det PMD | vacMode High vacuum | WD 16.4 mm | 200 µm | SK12-203

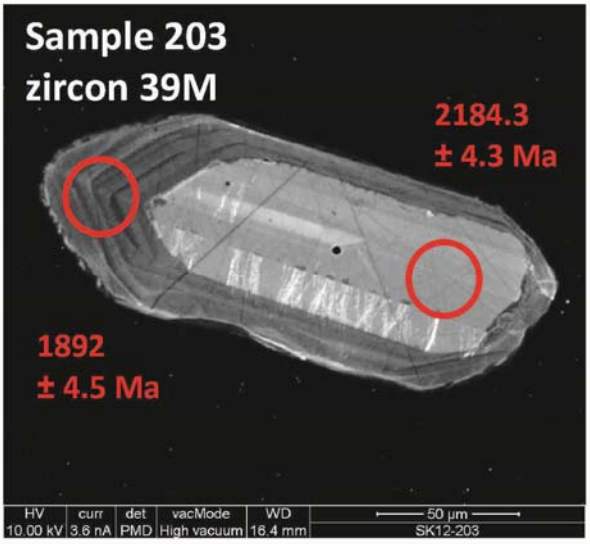
Sample 203
zircon 39M
2184.3
± 4.3 Ma
1892
± 4.5 Ma
HV 10.00 kV | curr 3.6 nA | det PMD | vacMode High vacuum | WD 16.4 mm | 50 µm | SK12-203

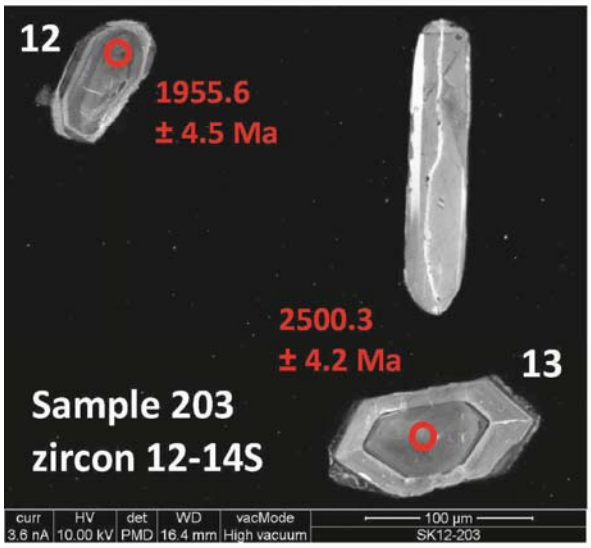
12
1955.6
± 4.5 Ma
2500.3
± 4.2 Ma
13
Sample 203
zircon 12-14S
curr 3.6 nA | HV 10.00 kV | det PMD | WD 16.4 mm | vacMode High vacuum | 100 µm | SK12-203

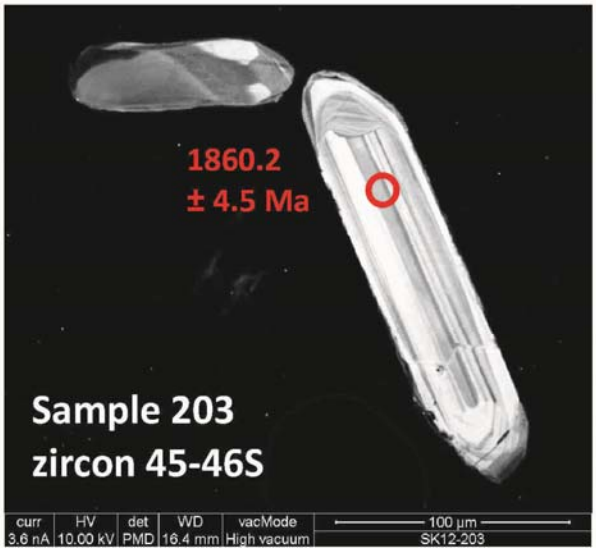
1860.2
± 4.5 Ma
Sample 203
zircon 45-46S
curr 3.6 nA | HV 10.00 kV | det PMD | WD 16.4 mm | vacMode High vacuum | 100 µm | SK12-203

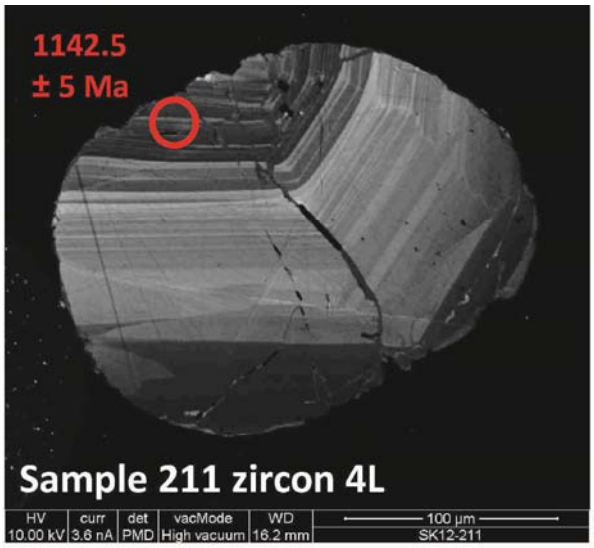
1142.5
± 5 Ma
Sample 211 zircon 4L
HV 10.00 kV | curr 3.6 nA | det PMD | vacMode High vacuum | WD 16.2 mm | 100 µm | SK12-211

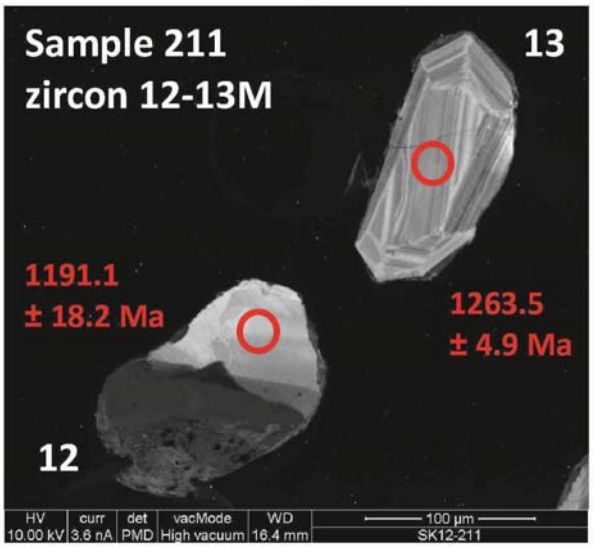
Sample 211
zircon 12-13M
13
1191.1
± 18.2 Ma
1263.5
± 4.9 Ma
12
HV 10.00 kV | curr 3.6 nA | det PMD | vacMode High vacuum | WD 16.4 mm | 100 µm | SK12-211

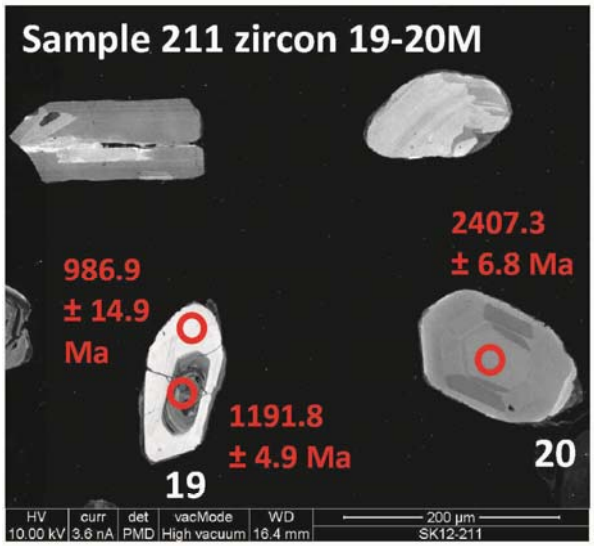
Sample 211 zircon 19-20M
2407.3
± 6.8 Ma
986.9
± 14.9
Ma
1191.8
± 4.9 Ma
19
20
HV 10.00 kV | curr 3.6 nA | det PMD | vacMode High vacuum | WD 16.4 mm | 200 µm | SK12-211

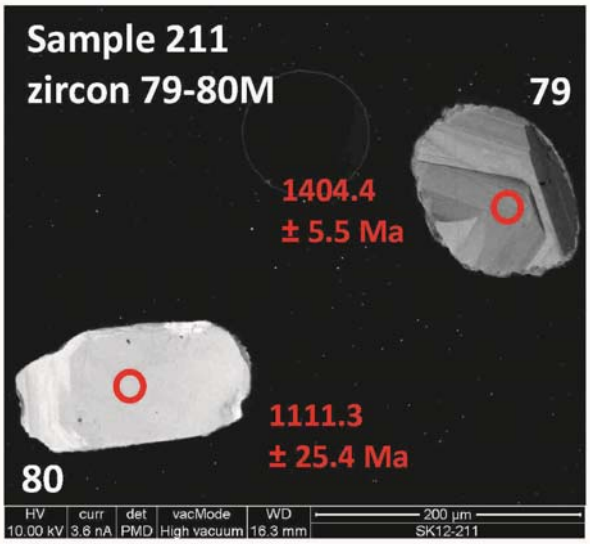
Sample 211
zircon 79-80M
79
1404.4
± 5.5 Ma
1111.3
± 25.4 Ma
80
HV 10.00 kV | curr 3.6 nA | det PMD | vacMode High vacuum | WD 16.3 mm | 200 µm | SK12-211

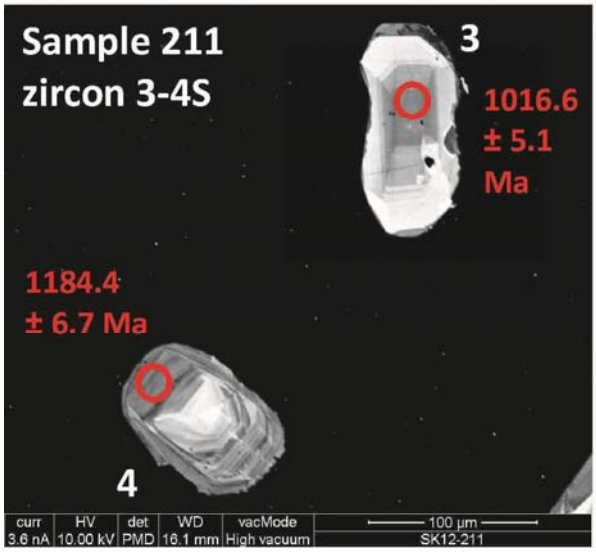
Sample 211
zircon 3-4S
3
1016.6
± 5.1
Ma
1184.4
± 6.7 Ma
4
curr 3.6 nA | HV 10.00 kV | det PMD | WD 16.1 mm | vacMode High vacuum | 100 µm | SK12-211

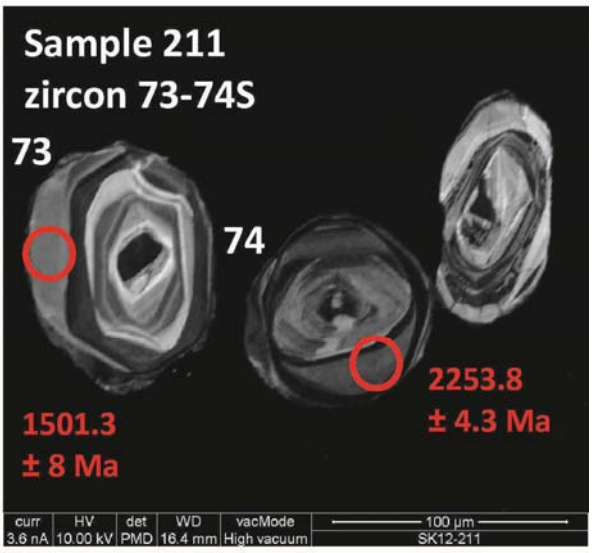
Sample 211
zircon 73-74S
73
74
2253.8
± 4.3 Ma
1501.3
± 8 Ma
curr 3.6 nA | HV 10.00 kV | det PMD | WD 16.4 mm | vacMode High vacuum | 100 µm | SK12-211

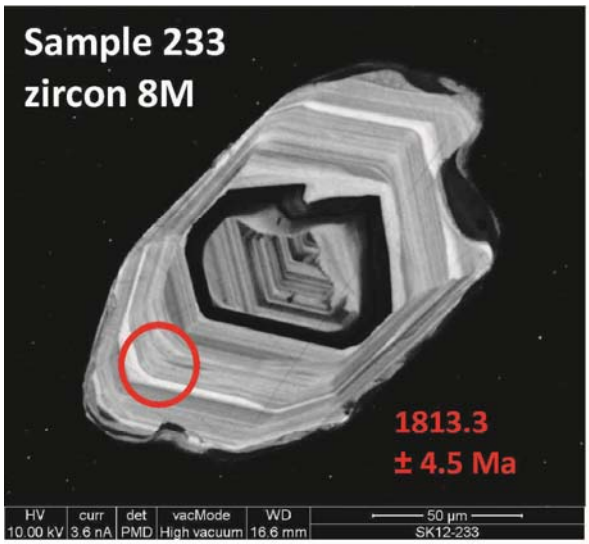
Sample 233
zircon 8M
1813.3
± 4.5 Ma
HV curr det vacMode WD 50 µm
10.00 kV 3.6 nA PMD High vacuum 16.6 mm SK12-233

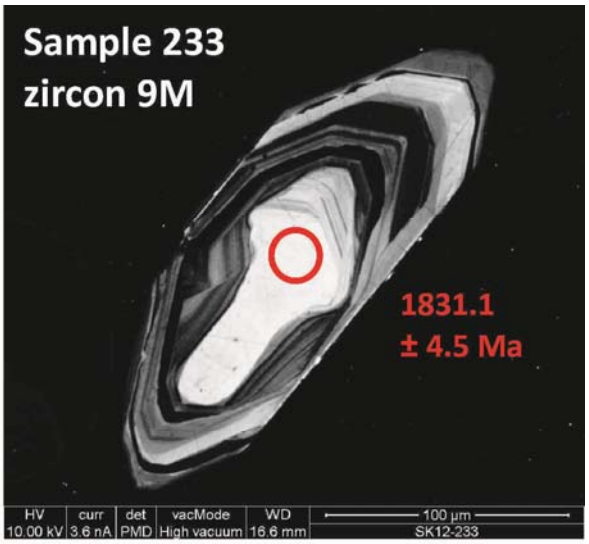
Sample 233
zircon 9M
1831.1
± 4.5 Ma
HV curr det vacMode WD 100 µm
10.00 kV 3.6 nA PMD High vacuum 16.6 mm SK12-233

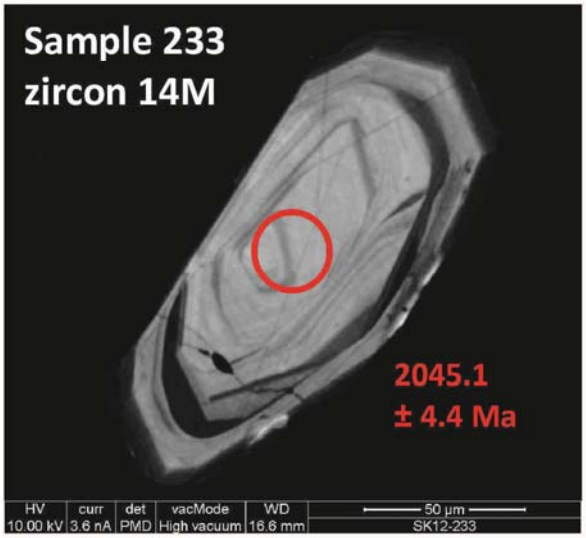
Sample 233
zircon 14M
2045.1
± 4.4 Ma
HV curr det vacMode WD 50 µm
10.00 kV 3.6 nA PMD High vacuum 16.6 mm SK12-233

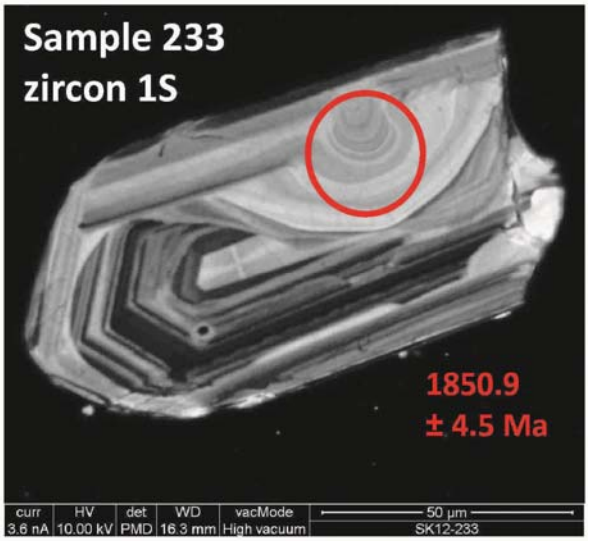
Sample 233
zircon 1S
1850.9
± 4.5 Ma
curr HV det WD vacMode 50 µm
3.6 nA 10.00 kV PMD 16.3 mm High vacuum SK12-233

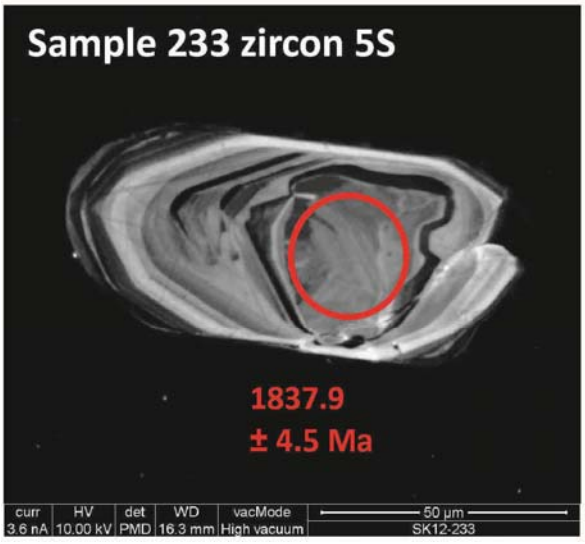
Sample 233 zircon 5S
1837.9
± 4.5 Ma
curr HV det WD vacMode 50 µm
3.6 nA 10.00 kV PMD 16.3 mm High vacuum SK12-233

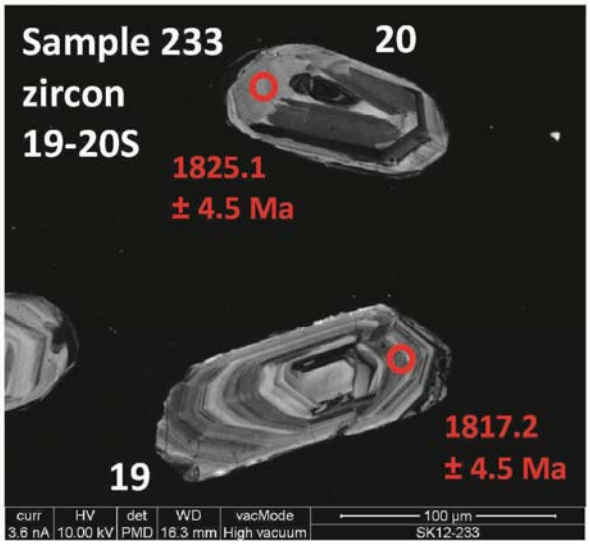
Sample 233
zircon
19-20S
20
1825.1
± 4.5 Ma
19
1817.2
± 4.5 Ma
curr HV det WD vacMode 100 µm
3.6 nA 10.00 kV PMD 16.3 mm High vacuum SK12-233

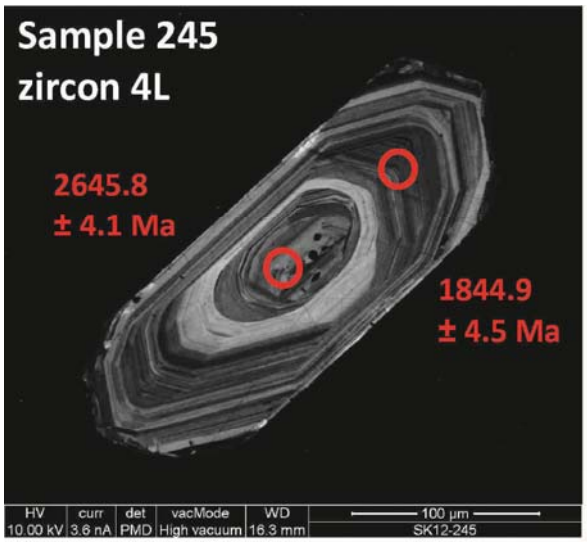
Sample 245
zircon 4L
2645.8
± 4.1 Ma
1844.9
± 4.5 Ma
HV 10.00 kV | curr 3.6 nA | det PMD | vacMode High vacuum | WD 16.3 mm | 100 µm | SK12-245

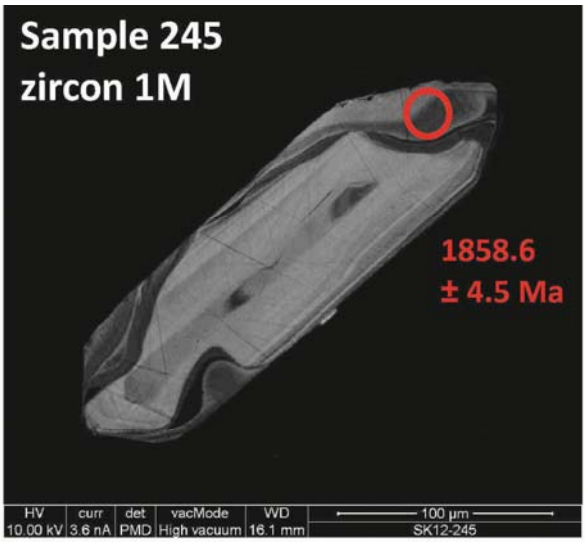
Sample 245
zircon 1M
1858.6
± 4.5 Ma
HV 10.00 kV | curr 3.6 nA | det PMD | vacMode High vacuum | WD 16.1 mm | 100 µm | SK12-245

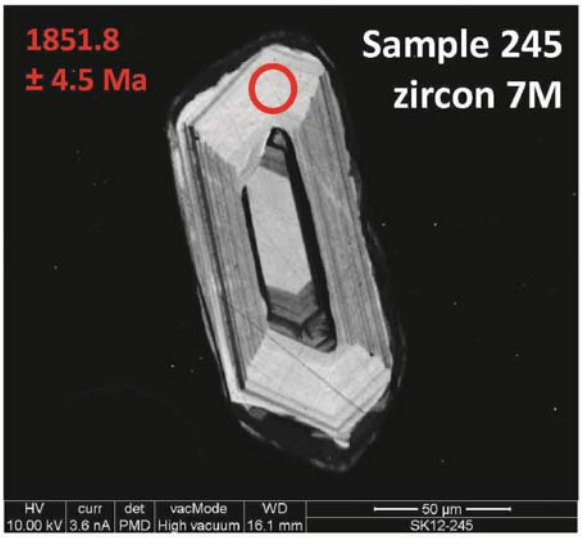
1851.8
± 4.5 Ma
Sample 245
zircon 7M
HV 10.00 kV | curr 3.6 nA | det PMD | vacMode High vacuum | WD 16.1 mm | 50 µm | SK12-245

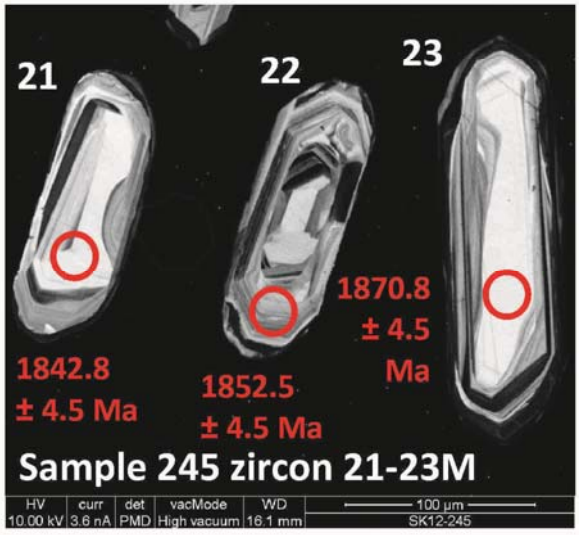
21
22
23
1870.8
± 4.5
Ma
1842.8
± 4.5 Ma
1852.5
± 4.5 Ma
Sample 245 zircon 21-23M
HV 10.00 kV | curr 3.6 nA | det PMD | vacMode High vacuum | WD 16.1 mm | 100 µm | SK12-245


Sample 245 zircon 38-39M
38
39
1865.5
± 4.5 Ma
1860.8
± 4.5 Ma
HV 10.00 kV | curr 3.6 nA | det PMD | vacMode High vacuum | WD 16.1 mm | 100 µm | SK12-245

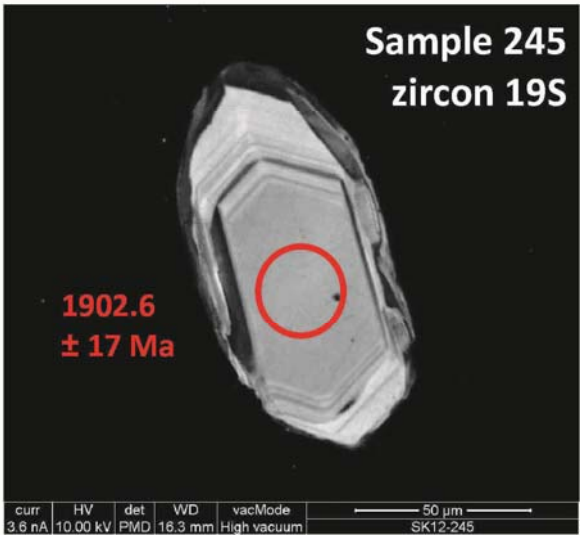
Sample 245
zircon 19S
1902.6
± 17 Ma
curr 3.6 nA | HV 10.00 kV | det PMD | WD 16.3 mm | vacMode High vacuum | 50 µm | SK12-245

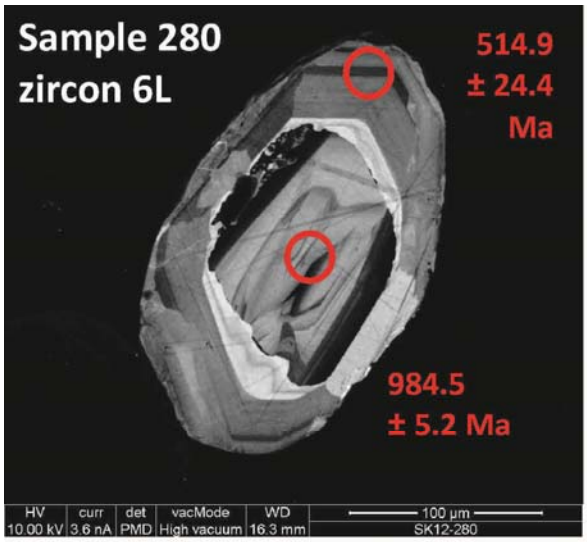
Sample 280
zircon 6L
514.9
± 24.4
Ma
984.5
± 5.2 Ma
HV curr det vacMode WD 100 µm
10.00 kV 3.6 nA PMD High vacuum 16.3 mm SK12-280

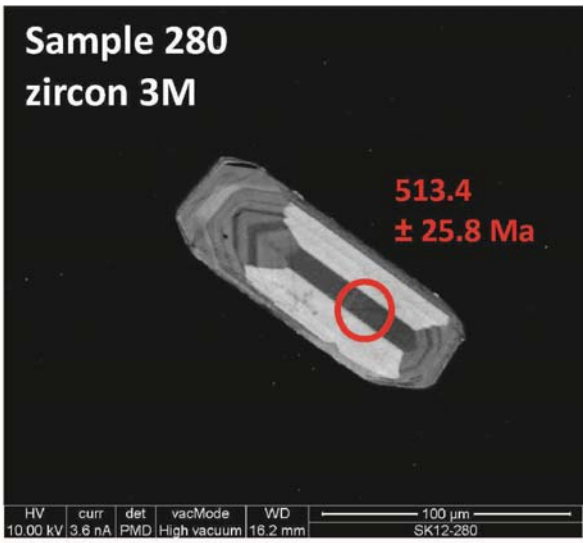
Sample 280
zircon 3M
513.4
± 25.8 Ma
HV curr det vacMode WD 100 µm
10.00 kV 3.6 nA PMD High vacuum 16.2 mm SK12-280

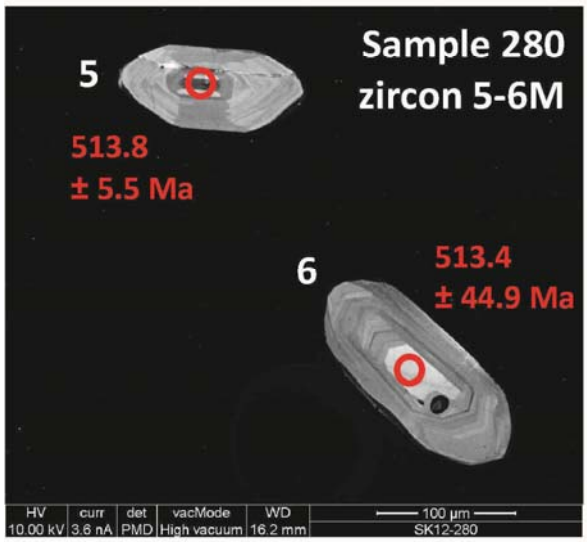
Sample 280
zircon 5-6M
5
513.8
± 5.5 Ma
6
513.4
± 44.9 Ma
HV curr det vacMode WD 100 µm
10.00 kV 3.6 nA PMD High vacuum 16.2 mm SK12-280

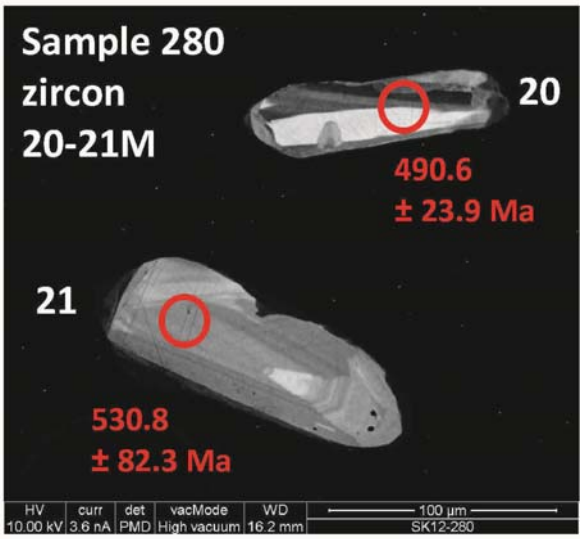
Sample 280
zircon
20-21M
20
490.6
± 23.9 Ma
21
530.8
± 82.3 Ma
HV curr det vacMode WD 100 µm
10.00 kV 3.6 nA PMD High vacuum 16.2 mm SK12-280


Sample 280
zircon 9S
1875.4
± 4.5 Ma
HV curr det vacMode WD 50 µm
20.00 kV 4.5 nA PMD High vacuum 16.4 mm SK12-280


Sample 280
zircon 10S
494.3
± 19.3 Ma
HV curr det vacMode WD 100 µm
20.00 kV 4.5 nA PMD High vacuum 16.4 mm SK12-280

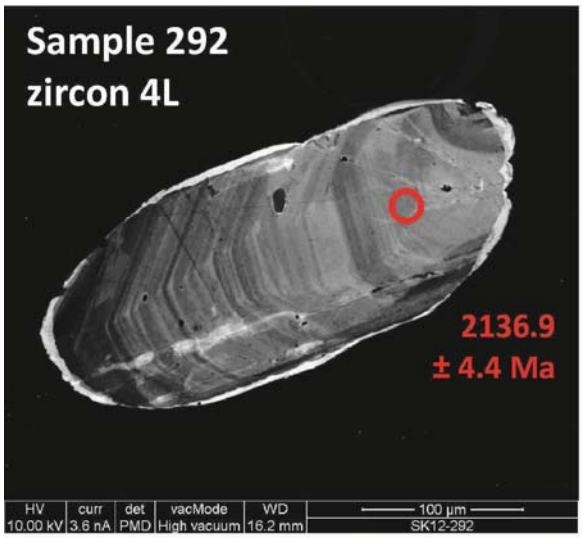
Sample 292
zircon 4L
2136.9
± 4.4 Ma
HV 10.00 kV | curr 3.6 nA | det PMD | vacMode High vacuum | WD 16.2 mm | 100 µm | SK12-292

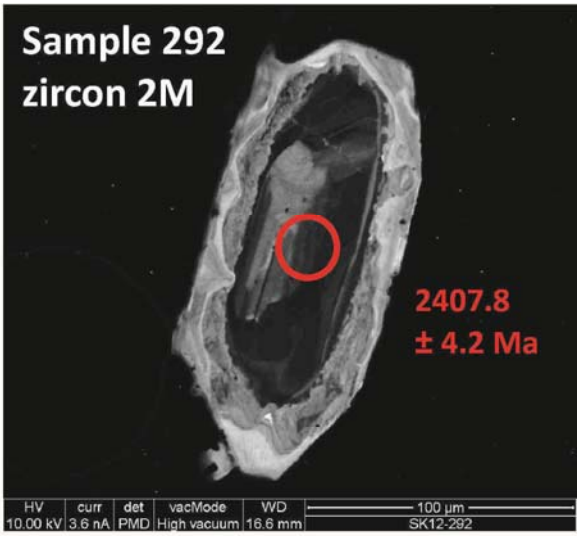
Sample 292
zircon 2M
2407.8
± 4.2 Ma
HV 10.00 kV | curr 3.6 nA | det PMD | vacMode High vacuum | WD 16.6 mm | 100 µm | SK12-292

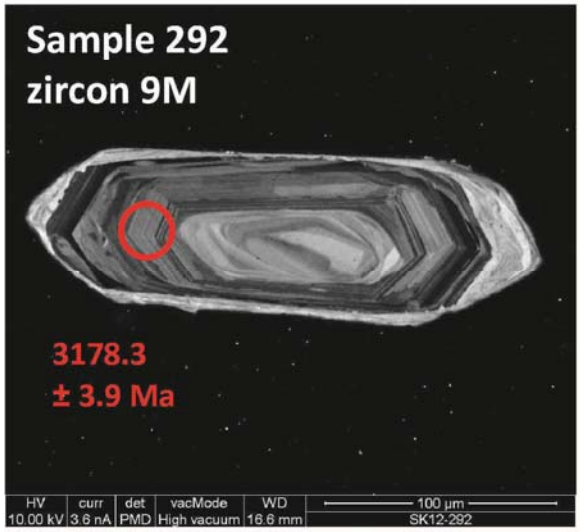
Sample 292
zircon 9M
3178.3
± 3.9 Ma
HV 10.00 kV | curr 3.6 nA | det PMD | vacMode High vacuum | WD 16.6 mm | 100 µm | SK12-292

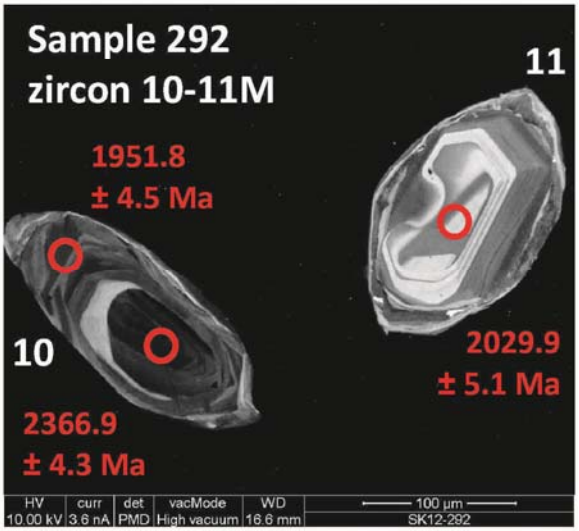
Sample 292
zircon 10-11M
11
1951.8
± 4.5 Ma
10
2366.9
± 4.3 Ma
2029.9
± 5.1 Ma
HV 10.00 kV | curr 3.6 nA | det PMD | vacMode High vacuum | WD 16.6 mm | 100 µm | SK12-292

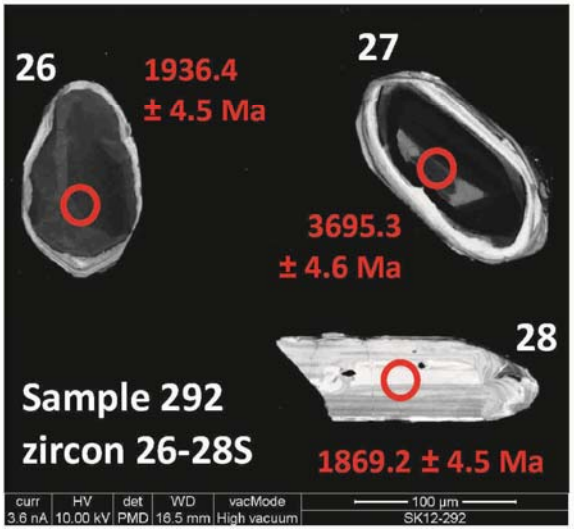
26
1936.4
± 4.5 Ma
27
3695.3
± 4.6 Ma
28
Sample 292
zircon 26-28S
1869.2 ± 4.5 Ma
curr 3.6 nA | HV 10.00 kV | det PMD | WD 16.5 mm | vacMode High vacuum | 100 µm | SK12-292

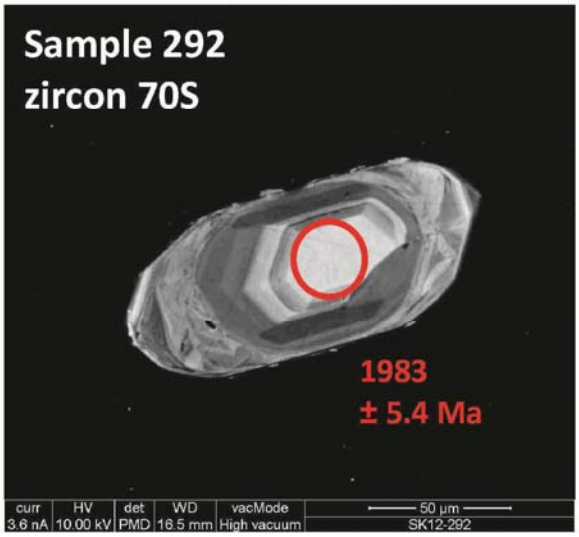
Sample 292
zircon 70S
1983
± 5.4 Ma
curr 3.6 nA | HV 10.00 kV | det PMD | WD 16.5 mm | vacMode High vacuum | 50 µm | SK12-292

S4. Full analytical conditions- Nu Plasma LA-MC-ICP-MS

U-Pb LA-MC-ICP-MS (zircon) isotope analyses at NIGL (BGS, Keyworth, UK)

Detrital zircon and orthogneiss samples were analysed at the NERC Isotope Geosciences Laboratory (NIGL) using a Nu Instruments, Nu Plasma HR multi-collector inductively coupled plasma mass spectrometer (MC-ICP-MS) equipped with a multi-ion-counting array. Instrumental parameters are shown in Table 1 and methodology is detailed in Thomas et al. (2010).

Rock samples were crushed using a jaw crusher and disk mill. Milled material was then sieved and material <355µm collected. The heavy material was separated from the light material using the Roger's table, which was then separated further using a Frantz magnetic separator. Subsequently the non-magnetic fraction was further separated using diodomethane heavy liquid separation. Finally zircons of varying sizes were picked from this heavy-non-magnetic fraction in ethanol. Samples were mounted in 25mm epoxy resin discs, polished to reveal an equatorial section of the mineral grains and imaged using a cathodoluminescence capability on the scanning electron microscope (SEM) FEI Quanta 600 ESEM, at the British Geological Survey, Keyworth.

Ablation was conducted using either a UP193FX (193nm) excimer or UP193SS (193nm) Nd:YAG laser ablation system (New Wave Research, UK) and an in-house designed low volume 'zircon ablation cell' (Horstwood et al. 2003) based on the design principles of Bleiner and Gunther (2001). Ablated sample material was transported from the laser cell into the MC-ICP-MS using a continuous flow of 0.8l/min of He gas. Operational parameters of the laser are detailed in Table 1.

The laser was fired using a repetition rate of 6Hz and a 25µm static spot size and a laser fluence of 1-2 $J.cm^{-2}$ or 3–4 $J.cm^{-2}$ due to core and rim uranium concentration variations and disparities between detrital grains. Typical ablation pit depths for fluence of 2-3 $J.cm^{-2}$ are of the order of 16µm as measured previously using an SEM.

Reference materials were analysed at regular intervals throughout the analytical session (typically 2-3 of each between each ablation run of unknowns). The internationally recognised 91500 zircon (Wiedenbeck et al. 1995) and GJ-1 (Jackson et al. 2004) were used as primary reference materials depending on the instrumental sensitivity and fluence used at the time. Plešovice (Sláma et al. 2008), GJ-1 and/or 91500 were variously used as appropriate secondary reference materials in order to validate the data for each day. As the data were collected in 21 separate analytical sessions spanning over a year, it has been possible to calculate a long-term reproducibility of ~2.5% (2SD) for Plešovice over the whole analytical period (14/03/2011- 28/06/2012) (Figure 1).

Pb-U uncertainties in the data tables are propagated for the reproducibility of the primary reference material, whilst uncertainties for Pb-Pb are propagated according to the 207Pb intensity of the measurement but limited at a minimum of 0.25% (1σ) to allow for reproducibility of the multi-ion counting measurement. All data were processed using an in-house spreadsheet calculation routine. The data are presented as Wetherill plots or $^{206}Pb/^{238}U$ age relative probability plots generated on all data <5% discordant using Isoplot 4.15 (Ludwig 2003). Due to slight discordance in some of the sample populations, ages are calculated as average $^{207}Pb/^{206}Pb$ ages with uncertainties as 2SD. The MSWD of the population is quoted and generally reflects excess scatter in the Pb/Pb data. Causes of this are assumed to be geological and poorly resolved, hence the preference for uncertainties at the level of 2SD.

Table 1: Laboratory & Sample Preparation (as per recommended reporting guidelines of CIRDLES http://cirdles.org)	
Laboratory name	NERC Isotope Geosciences Laboratory (NIGL), United Kingdom
Sample type/mineral	Detrital zircons/ orthogneisses
Sample preparation	Conventional mineral separation, 1 inch resin mount, 1um polish to finish
Imaging	CL, FEI Quanta 600 ESEM, 10nA, 15mm working distance
Laser ablation system	
Make, Model & type	UP193FX (193nm) Excimer / UP193SS (193nm) Nd:YAG laser ablation system (New Wave Research, UK)
Ablation cell & volume	In-house low volume ablation cell, volume c.3cm^3
Laser wavelength (nm)	193nm
Pulse width (ns)	3-4ns
Fluence (J.cm^{-2})	1-3 J.cm^{-2}
Repetition rate (Hz)	5Hz
Spot size (µm)	25µm
Sampling mode / pattern	Single spots
Carrier gas	100% He, Ar make-up gas combined using a Y-connector 50% along sample line.
Ablation duration (secs)	30secs
Cell carrier gas flow (l/min)	0.8l/min
ICP-MS Instrument	
Make, Model & type	Nu Instruments, Nu Plasma HR, MC-ICP-MS
Sample introduction	Ablation aerosol combined with co-aspiration of desolvated Tl-^{235}U tracer

RF power (W)	1300W
Make-up gas flow (l/min)	0.7l/min Ar
Detection system	mixed Faraday-multiple ion counting array
Masses measured	202-207, 235, 238
Integration time per peak (ms)	200ms
Total integration time per data point (secs)	1 sec
Detection Efficiency (%, element)	0.4% U
IC Dead time (ns)	6, 9 & 7ns IC0, IC1 & IC2 resp.
Data Processing	
Gas blank	30 second on-peak zero subtracted
Calibration strategy	91500 or GJ-1 used as primary reference material, Plesovice & GJ1 or 91500 used as secondaries.
Long-term reproducibility	2.5% (2SD) on Plesovice over a one year period
Reference Material info	91500 (Wiedenbeck et al 1995) Plesovice (Slama et al 2008) GJ1 $^{206}Pb/^{238}U$ 602.3 ± 1Ma, $^{207}Pb/^{206}Pb$ 609.2 ± 0.7Ma (in-house TIMS, unpublished)
Data processing package used / Correction for LIEF	Nu Instruments TRA software used to output data using average LIEF correction, In-house spreadsheet data processing used to reduce data and propagate uncertainties using the decay constants of Jaffey et al. 1971.
Mass discrimination	$^{207}Pb/^{206}Pb$ and $^{206}Pb/^{238}U$ normalised to reference material
Common-Pb correction, composition and uncertainty	No common-Pb correction applied
Uncertainty level &	Ages are quoted at 2sigma absolute, propagation is by quadratic

propagation	addition. Reproducibility and age uncertainty of reference material and common-Pb composition uncertainty are propagated.
Quality control / Validation	Plesovice – Weighted average $^{206}Pb/^{238}U$ age = 335 ± 1.5 (2SD, MSWD = 0.96) Figure 1 GJ-1 – Weighted average $^{206}Pb/^{238}U$ age = 603.47 ± 0.94 (95% confidence limit, MSWD = 1.4) Figure 2

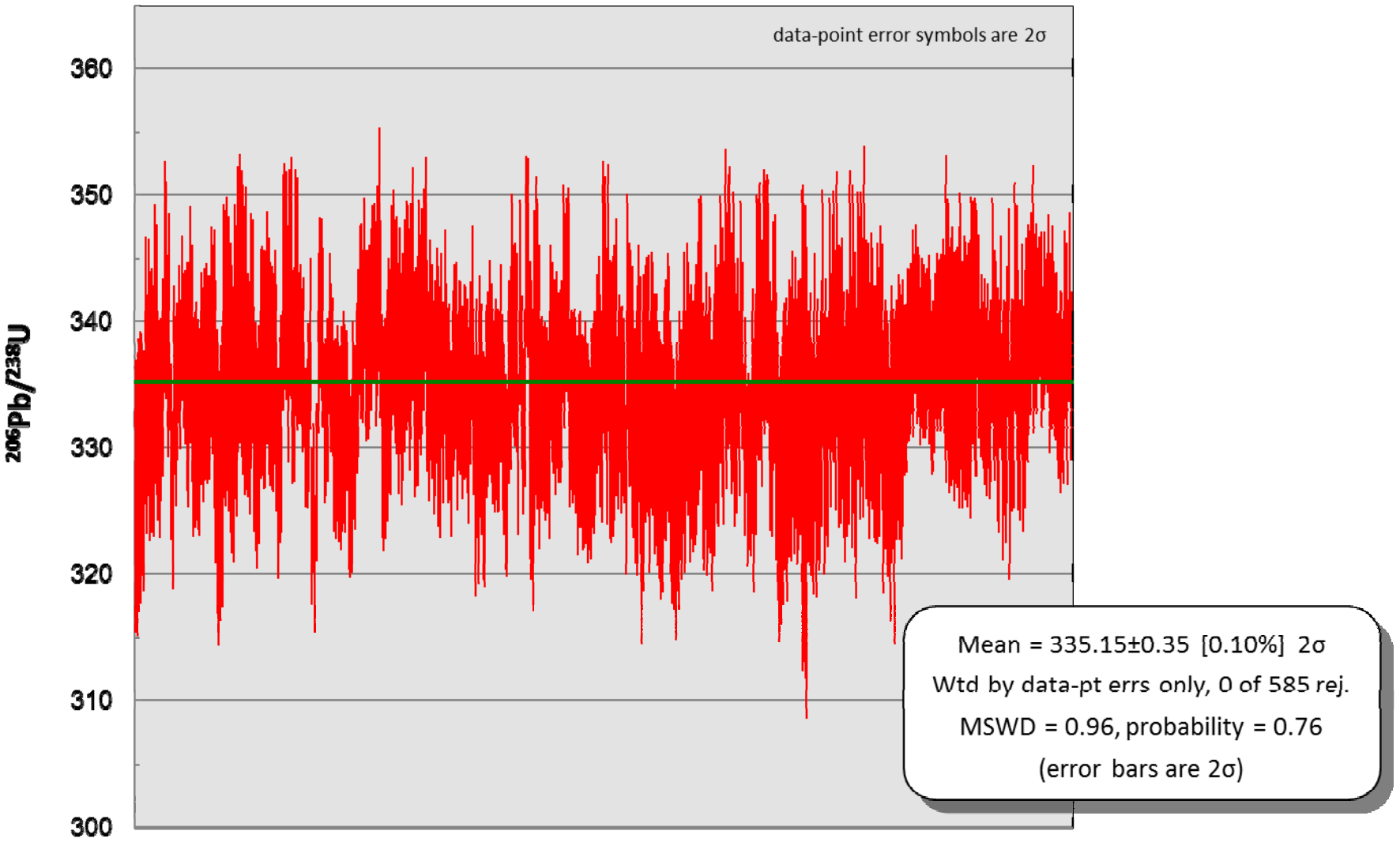

Figure 1: 2.5% (2SD) Long-term reproducibility of Plešovice (Sláma et al., 2008) 206Pb/238U age determined as validation over the analytical period 14.03.2011- 28.06.2012.

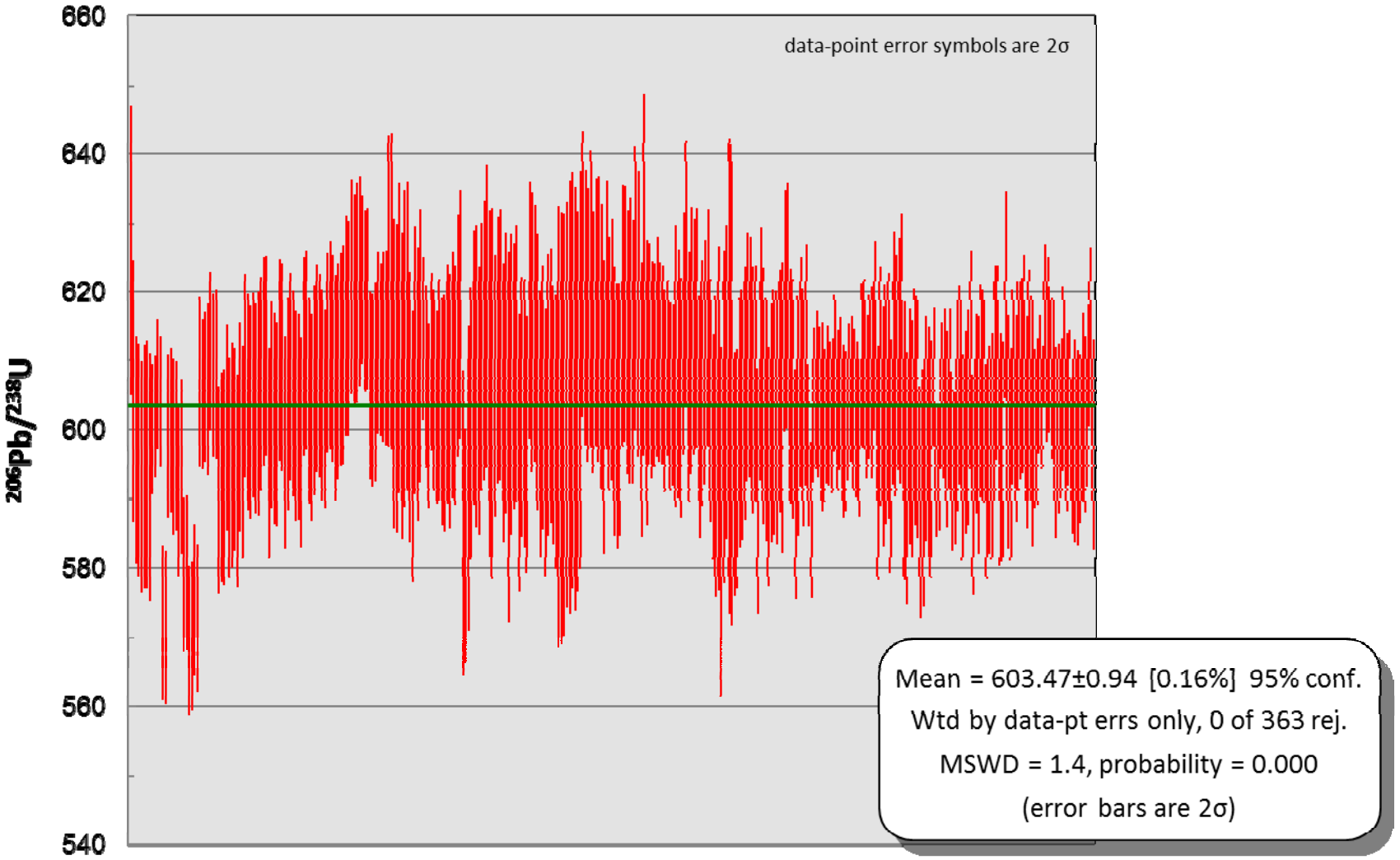

Figure 2: Long-term reproducibility of GJ-1 (Jackson et al., 2004) 206Pb/238U age determined as validation over the analytical period 14.03.2011-28.06.2012

S5. Full analytical conditions- AttoM LA-ICP-MS

Some zircons were analysed for U-Th-Pb geochronology using a Nu Instruments Attom HR single-collector inductively coupled plasma mass spectrometer (HR-ICP-MS). Laser ablation was performed using the equipment stated before. The ablation parameters were a 25µm static spot, a repetition rate of 5Hz, a fluence of 1.5 to 2.5 J/cm^2, a 15 second washout period between analyses, and a 30 second ablation time. The instrument was tuned to give ThO of <0.6%, and UO of <0.4%. Data processing used the time-resolved function on the Nu Instuments' software, an in-house Excel spreadsheet for data reduction and uncertainty propagation, and Isoplot for data presentation (Ludwig, 2003). All data are plotted at the 2σ confidence interval. Methodology followed that described in Thomas et al . (2013).

Laboratory & Sample Preparation	
Laboratory name	NERC Isotope Geosciences Laboratory
Sample type/mineral	Zircon
Sample preparation	Conventional mineral separation, 1 inch resin mount, 1/4µm polish to finish
Imaging	Cathodoluminescence
Laser ablation system	
Make, Model & type	New Wave Research UP193FX
Ablation cell & volume	In-house low volume ablation cell, volume c.3cm^3
Laser wavelength (nm)	193nm
Pulse width (ns)	3-4ns
Fluence (J.cm^{-2})	1.5-2.5 J.cm^{-2}
Repetition rate (Hz)	5Hz
Ablation duration (secs)	30secs
Ablation pit depth / ablation rate	~15µm pit depth, measured using an optical microscope
Spot size (m)	25µm
Sampling mode / pattern	Static spot ablation
Carrier gas	100% He, Ar make-up gas combined ca.50% along sample line.
Cell carrier gas flow (l/min)	0.8l/min
ICP-MS Instrument	
Make, Model & type	Nu Instruments Attom SC-SF-ICP-MS
Sample introduction	Free air aspiration via desolvator
RF power (W)	1300W
Make-up gas flow (l/min)	0.8l/min Ar
Detection system	Discrete dynode MassCom ion counter
Masses measured	202, 204, 206, 207, 208, 232, 235
Integration time per peak	200µs (202,204,206,208,232), 500µs (207,235)
Total integration time per reading (secs)	0.22 seconds

Detection Efficiency (%, element)	~0.27% for Uranium
IC Dead time (ns)	15ns
Data Processing	
Gas blank	60 second on-peak zero subtracted
Calibration strategy	91500, GJ1 & Plesovice (zircon); One used as primary reference material for normalization, and others for validation.
Reference Material info	91500 (1065 Ma; Wiedenbeck et al. 1995) GJ1 ($^{206}Pb/^{238}U$ 602.3 ± 1Ma, $^{207}Pb/^{206}Pb$ 609.2 ± 0.7Ma; in-house TIMS, – see also Jackson et al. 2004) Plesovice (337.13 Ma; Sláma et al., 2008)
Data processing package used / Correction for LIEF	Nu Instruments TRA acquisition software, in-house spreadsheet data processing
Mass discrimination	$^{207}Pb/^{206}Pb$ and $^{206}Pb/^{238}U$ normalised to reference material
Common-Pb correction, composition and uncertainty	No common-Pb correction applied
Uncertainty level & propagation	Ages in the data table are quoted at 2sigma absolute, propagation is by quadratic addition. Reproducibility of reference material is propagated.
Quality control / Validation	Plesovice – Weighted average $^{206}Pb/^{238}U$ age = 340 ± 2 (2SD, MSWD = 0.36) Figure 3 GJ-1 – Weighted average $^{206}Pb/^{238}U$ age = 601.5 ± 3.7 (2SD MSWD = 0.73) Figure 4

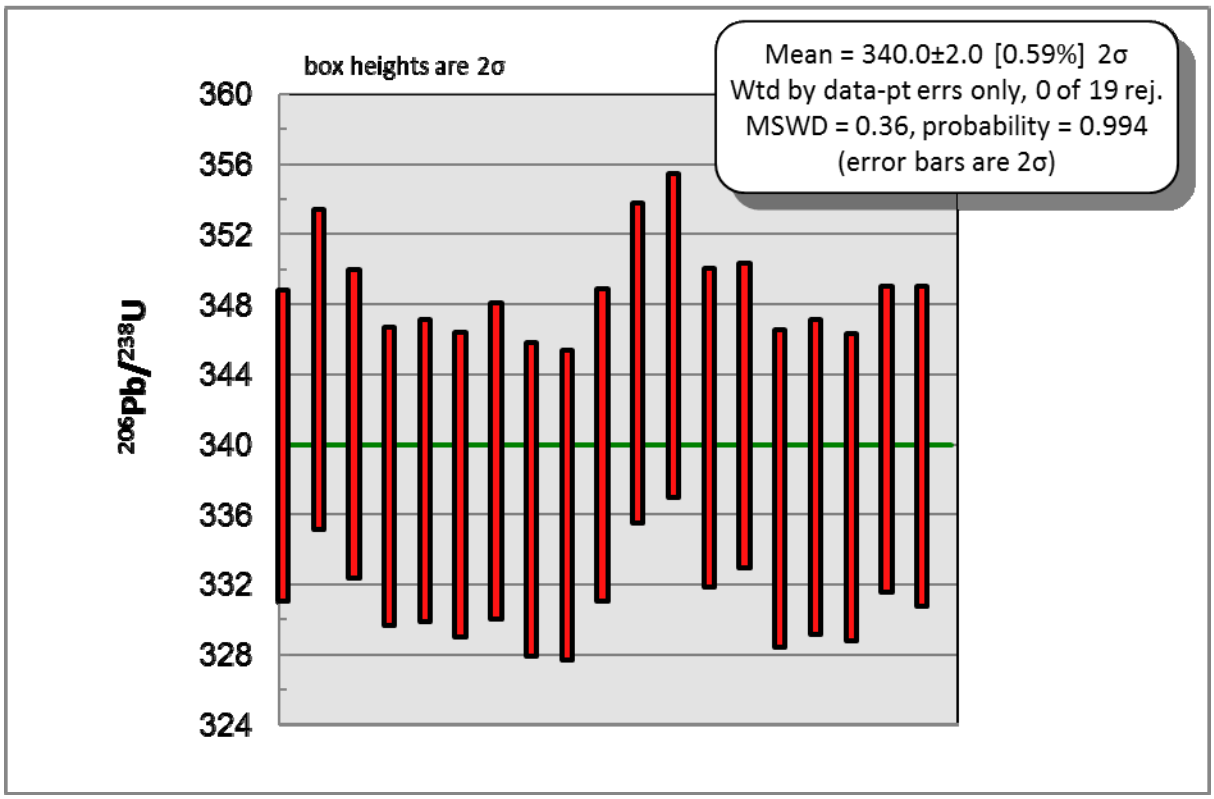

Figure 3: Reproducibility of Plešovice (Sláma et al., 2008) 206Pb/238U age determined as validation over the analytical period for Attom SC-SF-ICP-MS

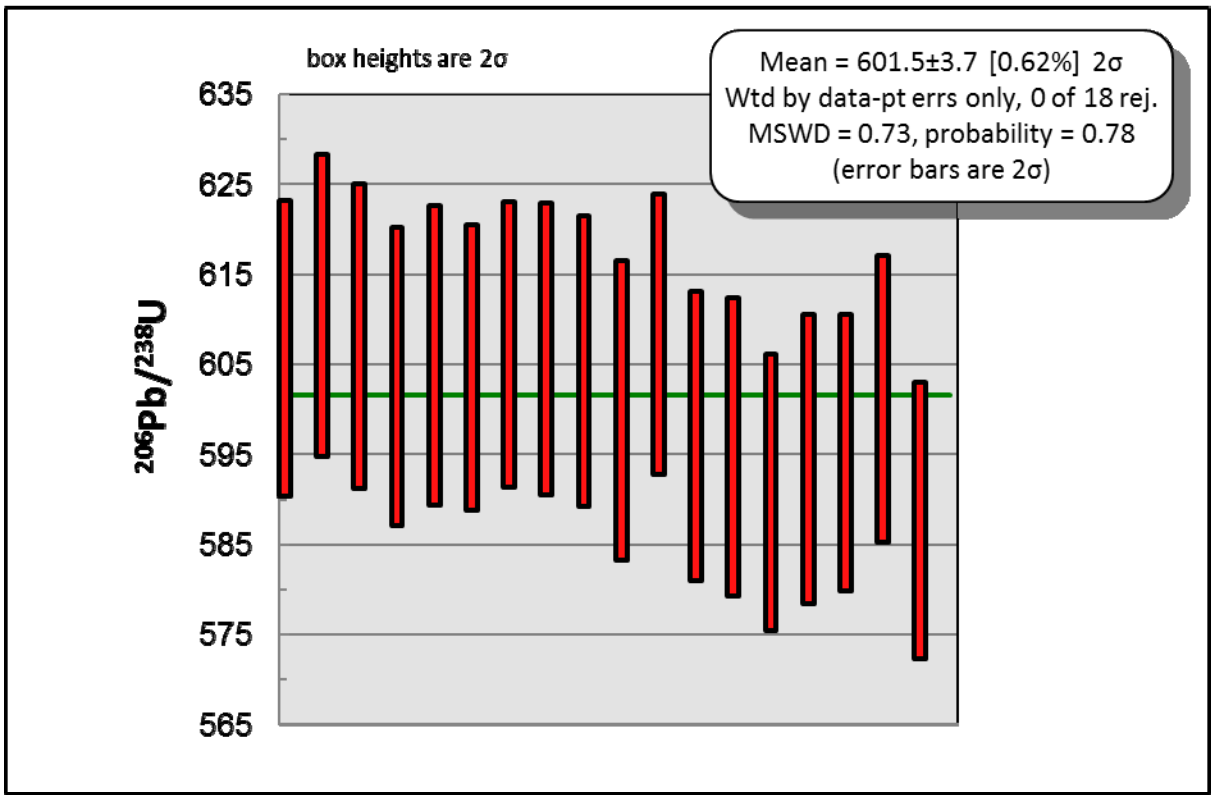

Figure 4: Reproducibility of GJ-1 (Jackson et al., 2004) 206Pb/238U age determined as validation over the analytical period for Attom SC-SF-ICP-MS

S6. Nd analytical techniques

Nd isotope analysis by thermal ionisation mass spectrometry (TIMS) at The Open University, UK.

Whole rock Nd isotopic ratios were determined by thermal ionisation mass spectrometry (TIMS) using a ThermoScientifc Triton at The Open University, UK.

Rock samples were crushed using a splitter, jaw crusher and agate ball mill. Approximately 100mg of powdered sample were dissolved and Nd isotopes were analysed using the following procedures (based on Pin and Zalduegui , 1997). Sm/Nd ratios were calculated from whole rock ICP-MS data. Total procedural blanks were spiked using ~5mg of SmNdLowDil spike.

Samples were digested using a standard HF - HNO_3 technique in a PFA Savillex® beaker. Prior to loading onto the ion exchange columns, samples were centrifuged to remove any residual graphite.

For Nd isotopic analyses, The REE elements were then separated from other elements, using a cation exchange resin (AG50w-x8). Neodymium was then separated from the other REE using Ln spec resin following the procedure outlined by Pin and Zalduegui (1997). Neodynium isotopes were analysed at the Open University using a ThermoFisher Triton thermal ionisation mass spectrometer (TIMS) in static mode. The sample was dissolved in dilute HCl and loaded onto one side of a double Re filament assemblage. After drying down, 1 μl of 0.01M H_3PO_4 was added to the filament and dried and the filament was then flashed at 1.8 A for a second. For both sample and standards about 150 ng of Nd was loaded. Most runs yielded ^{144}Nd intensities of 4 V and 270 ratios of 8.394 seconds were collected for each analysis. Samples were typically run at 4550-5100V (Ionising filament) and 1500-2300V (Evaporation filament), with a pyrometer temperature of between 1630-1750°C. Analyses were corrected for instrumental mass fractionation using the exponential fractionation law assuming a $^{146}Nd/^{144}Nd$ ratio of 0.7219 (O'Nions et al. 1977).

Repeat analyses of J&M standard gave 143Nd/144Nd ratios of 0.511838±0.000009 (n=5, 2σ) which compared to a long-term reproducibility on this machine of J&M of 0.511834±0.000012 (n=17, 2σ). Analysis of La Jolla standard gave 143Nd/144Nd ratios of 0.511864±0.00005 (2σ), which compared with a long term reproducibility on this machine of 0.511862±0.000011 (n=14, 2σ). Repeat analysis of the internationally recognised standard AGV-1 gave an average of 0.512417±0.000828 (n=4, 2σ), which is within error of the certified value (Raczek et al. 2003). Spiked total procedural blanks were analysed using the SEM on the TIMS. Total procedural blanks were negligible (between 27-98 pg).

147Sm/ 144Nd ratios were calculated from elemental ratios obtained from quadrupole ICP-MS. Repeat analyses of international standard AGV-1 gave a Nd accuracy of within 8% of certified values (USGS) and a Sm of within 5% of certified values. Repeat analyses of AGV-1 gave a precision of 3% (relative standard deviation) for both Nd and Sm measurements.

Epsilon Nd was calculated at time 0 using present day CHUR values of 0.512638 (Hamilton et al. 1983). Errors on εNd value are shown as a function of the error on $^{143}Nd/^{144}Nd$ measurement (from repeat analyses of J&M standard in epsilon units- 10000/0.511838*0.000009=0.17) which gives an average of 0.2 in epsilon units.

References

Bleiner, D. & Günther, D. 2001. Theoretical description and experimental observation of aerosol transport processes in laser ablation inductively coupled plasma mass spectrometry. *Journal of Analytical Atomic Spectrometry,* **16,** 449-456.

Hamilton, P. J., O'Nions, R. K., Bridgwater, D. & Nutman, A. 1983. Sm-Nd studies of Archaean metasediments and metavolcanics from West Greenland and their implications for the Earth's early history. *Earth and Planetary Science Letters,* **62,** 263-272.

Horstwood, M. S., Foster, G. L., Parrish, R. R., Noble, S. R. & Nowell, G. M. 2003. Common-Pb corrected in situ U–Pb accessory mineral geochronology by LA-MC-ICP-MS. *Journal of Analytical Atomic Spectrometry,* **18,** 837-846.

Jackson, S. E., Pearson, N. J., Griffin, W. L. & Belousova, E. A. 2004. The application of laser ablation-inductively coupled plasma-mass spectrometry to in situ U–Pb zircon geochronology. *Chemical Geology,* **211,** 47-69.

Jaffey, A., Flynn, K., Glendenin, L., Bentley, W. t. & Essling, A. 1971. Precision Measurement of Half-Lives and Specific Activities of^{235} U and^{238} U. *Physical Review C,* **4,** 1889.

O'Nions, R. K., Hamilton, P. J. & Evensen, N. M. 1977. Variations in143Nd/144Nd and87Sr/86Sr ratios in oceanic basalts. *Earth and Planetary Science Letters,* **34,** 13-22.

Pin, C. & Zalduegui, J. S. 1997. Sequential separation of light rare-earth elements, thorium and uranium by miniaturized extraction chromatography: Application to isotopic analyses of silicate rocks. *Analytica Chimica Acta,* **339,** 79-89.

Raczek, I., Jochum, K. P. & Hofmann, A. W. 2003. Neodymium and Strontium Isotope Data for USGS Reference Materials BCR-1, BCR-2, BHVO-1, BHVO-2, AGV-1, AGV-2, GSP-1, GSP-2 and Eight MPI-DING Reference Glasses. *Geostandards Newsletter,* **27,** 173-179.

Sláma, J., Košler, J., Condon, D. J., et al. 2008. Plešovice zircon—a new natural reference material for U–Pb and Hf isotopic microanalysis. *Chemical Geology,* **249,** 1-35.

Thomas, R., Jacobs, J., Horstwood, M., Ueda, K., Bingen, B. & Matola, R. 2010. The Mecubúri and Alto Benfica groups, NE Mozambique: aids to unravelling ca. 1 and 0.5 Ga events in the east African orogen. *Precambrian Research,* **178,** 72-90.

Thomas, R. J., Roberts, N. M. W., Jacobs, J., Bushi, A. M., Horstwood, M. S. A. & Mruma, A. 2013. Structural and geochronological constraints on the evolution of the eastern margin of the Tanzania Craton in the Mpwapwa area, central Tanzania. *Precambrian Research,* **224,** 671-689.

Wiedenbeck, M., Alle, P., Corfu, F., et al. 1995. Three natural zircon standards for U-Th-Pb, Lu-Hf, trace element and REE analyses. *Geostandards Newsletter,* **19,** 1-23.